Journal of Pediatric Surgery (2009) 44, 2253–2257

ELSEVIER

Journal of
Pediatric
Surgery

www.elsevier.com/locate/jpedsurg

PAPS papers

# Risks and benefits of ending of mass screening for neuroblastoma at 6 months of age in Japan

Tatsuro Tajiri[a,*], Ryota Souzaki[a], Yoshiaki Kinoshita[a], Sakura Tanaka[a], Yuhki Koga[b], Aiko Suminoe[b], Akinobu Matsuzaki[b], Toshiro Hara[b], Tomoaki Taguchi[a]

[a]*Department of Pediatric Surgery, Graduate School of Medical Sciences, Kyushu University, Fukuoka 812-8582, Japan*
[b]*Department of Pediatrics, Graduate School of Medical Sciences, Kyushu University, Fukuoka 812-8582, Japan*

Received 17 July 2009; accepted 31 July 2009

**Key words:**
Neuroblastoma;
Mass screening;
Genetics;
Biology

**Abstract**

**Purpose:** The mass screening (MS) for neuroblastoma (NB) at 6 months of age in Japan was discontinued in 2004. This study assessed the risks and benefits of MS based on an analysis of NB detected before or after discontinuation of MS in Japan.

**Methods:** The clinical features and Brodeur's genetic type based on *MYCN*, DNA ploidy, and other genetic aberrations were assessed in 113 NB patients (20 cases after and 93 cases [55 MS cases] before the discontinuation of MS) older than 6 months treated at one institution since 1985.

**Results:** The 20 patients with NBs detected after MS was discontinued ranged in age from 7 to 67 months, 12 patients were stage 4, and 11 patients would have been detected at 6 months of age if they had undergone MS. The Brodeur's genetic type of these 20 patients showed that 30% (6/20) were type 1 (low risk), 55% (11/20) were type 2A (intermediate risk), and 15% (3/20) were type 2B (high risk). Of 93 patients with NB detected before MS was discontinued, 60% (56/93) were type 1, 18% (17/93) were type 2A, and 22% (20/93) were type 2B. Among the type 2A patients, 82% (9/11) of the patients detected after MS was discontinued showed stage 4, whereas only 50% (9/18) of those diagnosed before MS was discontinued were stage 4. The genetic analysis using single nucleotide polymorphism (SNP) array for type 2A showed that the pattern of genetic aberration was equivalent in those detected either before or after MS was discontinued.

**Conclusions:** There was a decrease of type 1 and an increase of type 2A NB in patients after MS was discontinued in Japan. These results suggest that most of the type 1 detected by MS has regressed, and most of the type 2A detected by MS has appeared sporadically as advanced NB in patients older than 1 year.



Beginning in 1985, a nationwide mass screening program (MS) for neuroblastoma (NB) was conducted for 6-month-old infants throughout Japan [1,2]. More than 2000 Japanese children have been diagnosed with NB based on the MS at 6 months of age. The outcome of these patients has been excellent, and more than 97% of all such patients are alive [3,4]. The number of patients with NB has increased since the initiation of MS started. Likewise, the number of patients younger than 1 year as well as the number of cases with early stage NB has also increased. However, the number of advanced-stage NB patients older than 1 year has not

Presented at the 42nd Annual Meeting of the Pacific Association of Pediatric Surgeons, Hong Kong, China, May 10-14, 2009.

* Corresponding author. Tel.: +81 92 642 5573; fax: +81 92 642 5580.
*E-mail address:* taji@pedsurg.med.kyushu-u.ac.jp (T. Tajiri).

0022-3468/$ – see front matter © 2009 Elsevier Inc. All rights reserved.
doi:10.1016/j.jpedsurg.2009.07.050

substantially changed in several reports [5,6]. These findings imply that a number of tumors in this age group (6 months of age) have the capacity to either spontaneously regress or mature, and thus they may not be detected clinically.

Mass screening for NB at 6 months of age in Japan was discontinued in 2004. Most of the NBs detected by MS show a good prognosis [7], whereas only a few cases demonstrate an unfavorable outcome [8]. This study aims to assess the risk and benefit of MS based on an analysis of NB detected before or after the discontinuation of MS in Japan.

## 1. Materials and methods

The details of the MS protocol in Japan have been published elsewhere [9]. Briefly, the presence of urinary vanillylmandelic acid (VMA) and homovanillic acid (HVA) is measured by high-performance liquid chromatography.

Between 1985 and 2008, 113 NB patients older than 6 months were treated at our institution. Fifty-five of the 93 NBs detected before the discontinuation of MS (MS-positive cases) were detected through MS at 6 months of age, 27 cases (MS-negative cases) were detected in children older than 6 months sporadically in the cohort of children who underwent MS at 6 months of age, and 11 cases (nonscreened cases) were detected in children older than 6 months sporadically in the cohort of children who did not undergo MS at 6 months of age. Twenty cases in children older than 6 months were detected in the cohort of children who did not undergo MS after the discontinuation of MS.

The following clinical features were analyzed: age, initial symptom, the clinical stage (International Neuroblatoma Staging System), the site of the primary tumor, urinary VMA and HVA, the treatment, and the outcome of the patients.

The following biological features were also examined: MYCN amplification; DNA ploidy; other genetic aberrations such as 1p loss, 2p gain, 3p loss, 11q loss, and 17q gain; and the Shimada histology [10]. Consent was obtained from the patient's parents for tumor preservation and biological analysis before surgery. The *MYCN* amplification status was examined using the fluorescence in situ hybridization (FISH) method, quantitative polymerase chain reaction (PCR), and Southern blotting [11]. The 1p loss was determined by 2-color FISH method or SNP array. Other genetic aberrations such as the 3p loss, 11q loss, and the 17q gain were evaluated by SNP array. DNA ploidy was assessed using flow cytometry. The protocols used for FISH and quantitative PCR have been described in detail in previous reports [11-13]. SNP array experiments were done using Human CMV370-Duo (Illumina, San Diego, CA) according to the manufacturer's protocol. Genomic profiles were created using the Illumina Genome Viewer (IGV) and Chromosome Browser (ICV) of Illumina's BeadStudio2.0 software program. Based on these genetic features, all NBs were classified into 3 groups (type 1, type 2A, type 2B) using Brodeur's genetic type (BGT) [14]. Type 1 is triploid and does not have any MYCN amplification, 1p loss, 3p loss, 11q loss, or 17q gain. Type 2A is diploid, and at least one of other genetic aberration such 1p loss, 3p loss, 11q loss, and 17q gain. Type 2B is diploid and MYCN amplification. The statistical test of difference in each genetic

**Table 1** The clinical features of NB detected after the discontinuation of MS

| Case | Age (mo) | Stage (INSS) | Symptom | Primary site | Urinary VMA or HVA | Treatment | Outcome | Time from diagnosis (mo) |
|---|---|---|---|---|---|---|---|---|
| 1 | 13 | 2A | Free | Ad | Increase | Biopsy-chemo | CR | 58 |
| 2 | 10 | 1 | Free | Ad | Increase | Ope | CR | 47 |
| 3 | 25 | 4 | Fever, anemia | Ad | Increase | Biopsy-chemo-ope-SCT | CR | 39 |
| 4 | 8 | 4 | Free | Med | Increase | Biopsy-chemo-ope-chemo | CR | 37 |
| 5 | 18 | 1 | Stridor | Med | Increase | Ope-chemo | CR | 33 |
| 6 | 9 | 4 | Fever | Ad | Increase | Biopsy-chemo-SCT-ope | CR | 32 |
| 7 | 9 | 2B | Diarrhea | Ad | Increase | Biopsy-chemo-ope-chemo | CR | 25 |
| 8 | 7 | 3 | Free | Ad | Increase | Biopsy-chemo | CR | 21 |
| 9 | 42 | 4 | Fever, leg pain | Ad | Increase | Biopsy-chemo | PD | 20 |
| 10 | 13 | 4 | Exophthalmos | Ad | Increase | Biopsy-chemo | Undergoing | 18 |
| 11 | 49 | 4 | Abdominal mass | Ad | Increase | Ope-chemo | Undergoing | 17 |
| 12 | 45 | 4 | Leg pain | Ret | Increase | Biopsy-chemo | Undergoing | 16 |
| 13 | 67 | 4 | Cervical mass | Ad | Increase | Biopsy-chemo-ope-SCT | CR | 13 |
| 14 | 13 | 1 | Abdominal mass | Ad | Increase | Ope | CR | 11 |
| 15 | 8 | 1 | Free | Ad | Increase | Ope | CR | 10 |
| 16 | 57 | 4 | Abdominal mass | Ret | Increase | Biopsy-chemo | Undergoing | 8 |
| 17 | 14 | 3 | Opsoclonus-myoclonus | med | Increase | Ope-chemo | Undergoing | 8 |
| 18 | 21 | 4 | Fever, leg pain | Ad | Increase | Biopsy-chemo | Undergoing | 4 |
| 19 | 28 | 4 | Abdominal mass | Ad | Increase | Biopsy-chemo | Undergoing | 1 |
| 20 | 10 | 4 | Exophthalmos | Ad | Increase | Biopsy-chemo | Undergoing | 1 |

Ad indicates adrenal gland; med, mediastinum; ret, retroperitoneum; chemo, chemotherapy; ope, tumor extirpation; SCT, stem cell transplantation; CR, complete response; PD, progressive disease; INSS, International Neuroblatoma Staging System.

aberrance between NB before and after discontinuation of MS was analyzed with the $\chi^2$ and Fisher's Exact tests.

## 2. Results

### 2.1. Clinical features of 20 NBs detected in children older than 6 months sporadically in the cohort of children who did not undergo MS after the discontinuation of MS

The clinical characteristics of *20 NBs* detected sporadically in children older than 6 months in the cohort of children who did not undergo MS after discontinuation of MS are presented in Table 1. The age ranged from 7 to 67 months (median age, 13 months). There were 6 stage 1 or 2, 2 stage 3, and 12 stage 4 cases. Five free cases were detected by abdominal echo or chest x-ray conducted because of a nonrelated symptom. The primary tumor sites were the adrenal gland region in 15 cases and the nonadrenal gland region in 5 cases. In all 20 cases, the urinary VMA or HVA was elevated. Regarding the treatment of the patients younger than 12 months, in principle, the protocol of the Japanese Infantile Neuroblastoma study have been administered for patients younger than 12 months since 1994 [15]. Patients older than 1 year, in principle, have been treated based on the protocol of the Japan Study Group for Advanced Neuroblastoma for the patients older than 1 year with advanced neuroblastomas since 1998 [16]. Although the follow-up period was short, all of the patients are alive, and 11 of the 20 patients have demonstrated an event-free survival.

### 2.2. Biological features of 20 NBs detected sporadically in children older than 6 months in the cohort of children who did not undergo MS after the discontinuation of MS

The biological features of 20 NBs detected in children older than 6 months sporadically in the cohort of children who did not undergo MS after discontinuation of MS are presented in Table 2. Three (15%) of the 20 examined cases demonstrated an amplification of *MYCN* by FISH and quantitative PCR, in addition to the Southern blot method. Of the 20 cases, 14 (70%) had a diploid or tetraploid pattern based on flow cytometry. Of the 19 examined cases, 4 (21%) showed a 1p deletion by 2-color FISH method or SNP array. Fourteen cases were analyzed using an SNP array, and 4 showed 2p gain, 4 showed 3p loss, 7 showed 11q loss, and 6 showed 17q. Based on Shimada's histologic classification, 10 (53%) of the 19 examined tumors were considered to have an unfavorable histology. The BGT determined based on these genetic features showed that 6 patients were type 1 (low risk), 11 type 2A (intermediate risk), and 3 type 2B (high risk).

### 2.3. Comparison of NBs detected before and after the discontinuation of MS

Table 3 shows a comparison of the BGT for the NBs detected before and after the discontinuation of MS. The BGT for the 20 NBs detected after the discontinuation of MS was type 1 in 30% (6/20), type 2A in 55% (11/20),

**Table 2** The biological features of NB detected after the discontinuation of MS

| Case | The status of MYCN | | | DNA Ploidy | 1p loss | 2p gain | 3p loss | 11q loss | 17q gain | Shimada histology | BGT |
|---|---|---|---|---|---|---|---|---|---|---|---|
| | SB (copy no.) | FISH | PCR | | | | | | | | |
| 1 | 1 | No amp. | No amp. | TR | No | No | No | No | No | FH | Type 1 |
| 2 | 1 | No amp. | No amp. | TR | No | No | No | No | No | FH | Type 1 |
| 3 | 1 | No amp. | No amp. | D/T | No | No | Yes | Yes | Yes | UH | Type 2A |
| 4 | 1 | Gain | No amp. | D/T | No | Yes | Yes | Yes | No | FH | Type 2A |
| 5 | 1 | No amp. | No amp. | TR | No | No | No | No | No | FH | Type 1 |
| 6 | 40 | Amp. | Amp. | D/T | Yes | No | No | No | Yes | UH | Type 2B |
| 7 | 1 | No amp. | No amp. | TR | No | No | No | No | No | UH | Type 1 |
| 8 | 1 | No amp. | No amp. | TR | No | – | – | – | – | FH | Type 1 |
| 9 | 1 | Gain | No amp. | D/T | No | Yes | No | Yes | Yes | UH | Type 2A |
| 10 | 1 | Gain | Slight increase | D/T | Yes | Yes | Yes | Yes | No | UH | Type 2A |
| 11 | 1 | No amp. | No amp. | D/T | No | No | No | Yes | Yes | UH | Type 2A |
| 12 | 1 | No amp. | No amp. | D/T | – | – | – | – | – | – | Type 2A |
| 13 | 1 | No amp. | No amp. | D/T | No | Yes | No | Yes | Yes | UH | Type 2A |
| 14 | 1 | No amp. | No amp. | D/T | No | No | No | No | No | FH | Type 2A |
| 15 | 1 | No amp. | No amp. | TR | No | – | – | – | – | FH | Type 1 |
| 16 | 1 | No amp. | No amp. | D/T | No | No | Yes | Yes | Yes | UH | Type 2A |
| 17 | 1 | No amp. | No amp. | D/T | No | – | – | – | – | FH | Type 2A |
| 18 | 18 | Amp. | Amp. | D/T | No | – | – | – | – | UH | Type 2B |
| 19 | – | Amp. | Amp. | D/T | Yes | – | – | – | – | UH | Type 2B |
| 20 | – | Gain | Slight increase | D/T | Yes | – | – | – | – | FH | Type 2A |

SB indicates Southern blot; amp., amplification; TR, triploid; D/T, diploid or tetraploid.

**Table 3** Brodeur's genetic type of NB detected before or after the discontinuation of MS

| | BGT | | |
|---|---|---|---|
| | Type 1 | Type 2A | Type 2B |
| Before stop of MS (n = 93) | 56 (60%) | 17 (18%) | 20 (22%) |
| Screened cases (n = 82) | 55 (67%) | 11 (13%) | 16 (20%) |
| MS-positive cases (n = 55) | 49 (89%) | 4 (7%) | 2 (4%) |
| MS-negative cases (n = 27) | 6 (22%) | 7 (26%) | 14 (52%) |
| Nonscreened cases (n = 11) | 1 (9%) | 6 (55%) | 4 (36%) |
| After stop of MS (n = 20) | 6 (30%) | 11 (55%) | 3 (15%) |

Screened cases, NB detected in the cohort of children who underwent MS at 6 months of age; MS-positive cases, NB detected through MS at 6 months of age; MS-negative cases, NB detected at more than 6 months of age sporadically in the cohort of children who underwent MS at 6 months of age; nonscreened cases, NB detected at more than 6 months of age sporadically in the cohort of children who did not undergo MS at 6 months of age.

and type 2B in 15% (3/20). In contrast, in the 93 NBs detected before the discontinuation of MS, 60% (56/93) were type 1, 18% (17/93) type 2A, and 22% (20/93) type 2B. In the 55 MS-positive cases among these 93 NBs, 89% (49/55) were type 1, 7% (4/55) type 2A, and 4% (2/55) type 2B. In the 27 MS-negative cases among the 93 NBs, 22% (6/27) were type 1, 26% (7/27) type 2A, and 52% (14/27) type 2B. In the 11 nonscreened cases among these 93 NBs, 9% (1/11) were type 1, 55% (6/11) type 2A, and 36% (4/11) type 2B. In summary, there was a decrease of type 1 and an increase of type 2A NB in patients detected after MS was discontinued.

The clinical stage of type 2A NB before or after the discontinuation of MS is shown in Table 4. Twenty-eight percent was stage I (5/18) NB before the discontinuation of MS, whereas only 1% (1/11) was stage I NB after the discontinuation of MS. However, 50% (9/18) was stage 4 NB before the discontinuation of MS, whereas 82% (9/11) was stage 4 NB after the discontinuation of MS.

The genetic aberrations of type 2A NB before or after the discontinuation of MS are summarized in Table 5. The genetic aberrations of 8 type 2A NBs before the discontinuation of MS and 8 type 2A NBs after discontinuation of MS were analyzed using an SNP array. The significant difference was not observed between NB treated before and after discontinuation of MS in each genetic aberrance (1p loss, 2p gain, 3p loss, 11q loss, 17q gain), respectively.

**Table 4** Clinical stage of type 2A NB

| INSS | Before stop of MS (n = 18) | After stop of MS (n = 11) |
|---|---|---|
| Stage 1 | 5 (28%) | 1 (1%) |
| Stage 2A | 1 | 0 |
| Stage 2B | 1 | 0 |
| Stage 3 | 2 | 1 |
| Stage 4 | 9 (50%) | 9 (82%) |

**Table 5** Genetic aberrations of type 2A NB

| BGT | Before stop of MS (n = 8) | After stop of MS (n = 8) | *P* |
|---|---|---|---|
| 1p loss | 2 (25%) | 1 (13%) | NS |
| 2p gain | 3 (38%) | 3 (38%) | NS |
| 3p loss | 4 (50%) | 4 (50%) | NS |
| 11q loss | 6 (75%) | 7 (88%) | NS |
| 17q gain | 7 (88%) | 5 (63%) | NS |

NS indicates not significant.

## 3. Discussion

Most of the NBs detected by MS have a good prognosis. The purpose of MS at 6 months of age was to decrease the number of advanced-stage NB patients older than 1 year and mortality because of NB. Regrettably, this goal was not confirmed by several studies [6]. However, at least 17% of the NBs detected by MS have one or more biologically unfavorable factors and might thus have a higher risk of recurrence than in patients without such biologically unfavorable factors in our previous study [17]. Some of these tumors, which have one or more biologically unfavorable factors, may progress and eventually be fatal, if they are not detected by 6 months of age and, as a result, do not undergo any immediate surgical intervention with or without additional treatment. Furthermore, the analysis of large cohort in Japan recently reported that the mortality rate from NB in children who were screened at 6 months was lower than that in the prescreening cohort [18].

In the present study, 14 cases (60%) of 20 NBs detected sporadically in children older than 6 months in the cohort of children who did not undergo MS after the discontinuation of MS were advanced-stage NB (stage 3, 4). Furthermore, in all 20 cases, the urinary VMA or HVA was elevated. If the patients younger than 15 months already had a small tumor that secreted VMA or HVA at 6 months of age, 11 cases of 20 NBs would have been detected at 6 months of age if they underwent MS.

The analysis of BGT for NB before and after the discontinuation of MS in the present study showed a decrease of type 1 NB and an increase of type 2A NB in NB cases detected sporadically after the discontinuation of MS in Japan. Of type 2A NBs, the number of patients with stage 4 NB after the discontinuation of MS was more than that of patients with stage 4 NB before the discontinuation of MS. The rate of type 2A NB (55%) in the 20 NBs diagnosed after the discontinuation of MS was higher than that (26%) of the 27 MS-negative cases detected before the discontinuation of MS and almost equal to that (55%) of the 11 nonscreened cases before the discontinuation of MS. These results suggest

that most of the type 1 NBs detected by MS regressed and were not detected sporadically, and most of the type 2A NBs detected by MS were detected sporadically as advanced NB at more than 1 year of age after the discontinuation of MS. Another possibility is that the type 1 NBs detected by MS have intratumoral genetic heterogeneity, which is associated with some type 2A NB cells. In the present study, the pattern of genetic aberrations for type 2A NBs before discontinuation of MS and type 2A NBs after discontinuation of MS are quite similar. If type 1 NBs with the intratumoral genetic heterogeneity of type 2B NB cells are not detected during MS at 6 months of age, the type 2A NB cells of these tumors may progress and present sporadically as type 2A NB with advanced stage at more than 1 year of age.

As the present study is not a population-based study, and includes only a short follow-up period, the difference in the mortality rate and accurate incidence rate of NBs detected before and after the discontinuation of MS is unclear. This study is a preliminary report of the experience in Japan of managing NB after the discontinuation of MS. A future analysis of the population-based incidence of sporadically detected NB after the discontinuation of MS and the detailed evaluation for the biology of a large number of NB detected after the discontinuation of MS are necessary to elucidate the risks and benefits of MS at 6 months of age in Japan.

## Acknowledgment

The English language in the article was reviewed by Brian Quinn (Editor-in-Chief, Japan Medical Communication).

## References

[1] Sawada T, Kidowaki T, Sakamoto I, et al. Neuroblastoma: mass screening for early detection and its prognosis. Cancer 1984;53: 2731-5.

[2] Bessho F, Hashizume K, Nakajo T, et al. Mass screening in Japan increased the detection of infants with neuroblastoma without a decrease in cases in older children. J Pediatr 1991;119:237-41.

[3] Matsumura T, Shikata T, Sawada T. Treatment modality for neuroblastoma infants in Japan: retrospective analysis and future directions. Proceeding of the 31st American Society of Clinical Oncology. J Clin Oncol 1995;14:456.

[4] Suita S, Zaizen Y, Sera Y, et al. Mass screening for neuroblastoma: quo vadis? A 9-year experience from the Pediatric Oncology Study Group of the Kyushu area in Japan. J Pediatr Surg 1996;31:555-8.

[5] Suita S, Tajiri T, Akazawa K, et al. Mass screening for neuroblastoma at 6 months of age: difficult to justify. J Pediatr Surg 1998;33:1674-8.

[6] Yamamoto K, Ohata S, Ito E, et al. Marginal decrease in mortality and marked increase in incidence as a result of neuroblastoma screening at 6 months of age: cohort study in seven prefectures in Japan. J Clin Oncol 2002;20:1209-14.

[7] Suita S. Mass screening for neuroblastoma in Japan: lessons learned and future directions. J Pediatr Surg 2002;37:949-54.

[8] Tajiri T, Suita S, Takamatsu H, et al. Clinical and biologic characteristics for recurring neuroblastoma at mass screening cases in Japan. Cancer 2001;15:349-53.

[9] Suita S, Zaizen Y, Yano H, et al. How to deal with advanced cases neuroblastoma detected by mass screening: a report from the pediatric oncology study group of the Kyushu area of Japan. J Pediatr Surg 1994;29:599-603.

[10] Shimada H, Chatten J, Newton Jr WA, et al. Histopathologic prognostic factors in neuroblastic tumors: definition of subtypes of ganglioneuroblastoma and an age-linked classification of neuroblastomas. J Natl Cancer Inst 1984;73:405-16.

[11] Tanaka S, Tajiri T, Suita S, et al. Clinical significance of a highly sensitive analysis for gene dosage and the expression level of *MYCN* in neuroblastoma. J Pediatr Surg 2004;39:63-8.

[12] Tajiri T, Shono K, Tanaka S, et al. Evaluation of genetic heterogeneity in neuroblastoma. Surgery 2002;131:283-7.

[13] Tajiri T, Tanaka S, Shono K, et al. Quick quantitative analysis of gene dosages associated with prognosis in neuroblastoma. Cancer Lett 2001;166:89-94.

[14] Brodeur GM. Neuroblastoma: biological insights into a clinical enigma. Nat Rev Cancer 2003;3:203-16.

[15] Iehara T, Hosoi H, Akazawa K, et al. MYCN gene amplification is a powerful prognostic factor even in infantile neuroblastoma detected by mass screening. Br J Cancer 2006;94:1510-5.

[16] Kaneko M, Tsuchida Y, Uchino J. Treatment results of advanced neuroblastoma with the First Japanese Study Group Protocol. J Pediatr Hematol/Oncol 1999;21:190-7.

[17] Suita S, Tajiri T, Higashi M, et al. Insights into infant neuroblastomas based on an analysis of neuroblastomas detected by mass screening at 6 months of age in Japan. Eur J Pediatr Surg 2007;17:23-8.

[18] Hiyama E, Iehara T, Sugimoto T, et al. Effectiveness of screening for neuroblastoma at 6 months of age: a retrospective population-based cohort study. Lancet 2008;371:1173-80.

Cancer Science
The official journal of the Japanese Cancer Association

# The expression of dipeptidyl peptidase IV (DPPIV/CD26) is associated with enhanced chemosensitivity to paclitaxel in epithelial ovarian carcinoma cells

Hiroaki Kajiyama,[1] Kiyosumi Shibata, Kazuhiko Ino, Shigehiko Mizutani, Akihiro Nawa and Fumitaka Kikkawa

Department of Obstetrics and Gynecology, Nagoya University Graduate School of Medicine, Nagoya, Japan

(Received May 6, 2009/Revised September 3, 2009; September 22, 2009/Accepted September 24, 2009/Online publication November 16, 2009)

**Dipeptidyl peptidase IV (DPPIV/CD26) is a multifunctional cell surface aminopeptidase that is widely expressed in different cell types. Recent studies have suggested that DPPIV plays an important role in tumor progression in several human malignancies. In the current study, we investigated the role of DPPIV in paclitaxel resistance in epithelial ovarian carcinoma (EOC) cells. We first examined the correlation between expression levels of DPPIV and sensitivity to paclitaxel in various EOC cell lines. Subsequently, to clarify the cellular functions of DPPIV, we investigated the role of this molecule in the sensitivity of EOC to paclitaxel *in vitro* and *in vivo* using stably DPPIV-transfected EOC cells. We identified a positive correlation between DPPIV expression and paclitaxel sensitivity in various EOC cell lines. In addition, we observed a significant increase in the paclitaxel sensitivity of DPPIV-overexpressing EOC cells. Furthermore, no apparent alteration in paclitaxel sensitivity was noted by the addition of a specific inhibitor of DPPIV activity in DPPIV-transfected or natively DPPIV-overexpressing EOC cells. In a subcutaneous murine model treated with paclitaxel, on Day 39, the tumor size of the DPPIV-transfected cell-inoculated group was as large as that of the vector-transfected cell-inoculated group. In contrast, on Day 61, the former was smaller than the latter. The present findings show that DPPIV may be involved in the increased sensitivity to paclitaxel of EOC cells regardless of the involvement of DPPIV activity. (*Cancer Sci* 2010; 101: 347–354)**

Dipeptidyl peptidase IV (DPPIV) is a cell surface aminopeptidase which was originally characterized as a T-cell differentiation antigen (CD26),[1] and it has been reported to be present on epithelial cells of various tissues, including the lung, liver, kidney, intestine, prostate, and placenta.[2–4] Since DPPIV cleaves amino-terminal dipeptides from polypeptides with either L-proline or L-alanine in position 2, this enzyme is capable of degrading various bioactive peptides, cytokines, and several chemokines such as stromal cell-derived factor-1α (SDF-1α) or RANTES (regulated on activation, normal T-cell expressed, and secreted).[3,5,6] Therefore, a variety of reports have shown that DPPIV is involved in various cellular processes such as the regulation of immune-system-mediated responses, signal transduction, and interaction with molecules of the extracellular matrix.[7,8] In addition, a number of studies have provided evidence indicating that DPPIV may play a role in tumor suppression including an antiproliferative effect, and decreased invasive ability.[9–12] Moreover, a recent report from Aytac *et al.* showed that leukemic T cells overexpressing DPPIV, through its associated enzyme activity, displayed enhanced sensitivity to doxorubicin, associated with the disruption of cell cycle-related events.[13] Furthermore, Sato *et al.* demonstrated that DPPIV enhanced sensitivity to apoptosis induced by doxorubicin and etoposide with increased susceptibility to the mitochondrial pathway of apoptosis and enhanced topoisomerase II alpha expression.[14]

Epithelial ovarian carcinoma (EOC) is the leading cause of mortality among cancers of the female reproductive system.[15] The majority of patients with EOC have advanced intraperitoneal metastatic disease at diagnosis since this carcinoma frequently remains clinically silent. Today, paclitaxel-platinum-based chemotherapy has become the standard regimen for EOC worldwide. Nevertheless, despite the comparatively high-level sensitivity of EOC to paclitaxel, the prognosis of advanced or recurrent cases remains poor since most deaths are the result of metastasis that is refractory to these chemotherapeutic agents. To overcome such paclitaxel resistance, a variety of additional molecular-targeting therapies combined with paclitaxel have been investigated.[16,17] However, the detailed mechanism underlying the resistance remains unclear, and the effect of combined treatment is not satisfactory.

Previously, we demonstrated that DPPIV expression in EOC cell lines was negatively correlated with the invasive potential. In addition, DPPIV overexpression in EOC cells induced a marked change in the cellular morphology from a fibroblastic to an epithelioid pattern and a significant decrease in the invasive potential *in vitro* and *in vivo*.[10] In the current study, we focused on the association of DPPIV with the susceptibility of EOC to paclitaxel. We first examined the correlation between expression levels of DPPIV and sensitivity to paclitaxel in various EOC cell lines. Subsequently, to clarify the cellular functions of DPPIV, we investigated the role of this molecule in the sensitivity of EOC to paclitaxel *in vitro* and *in vivo* using stably DPPIV-transfected EOC cells. Herein, the possible application of this enzyme as a means of enhancing the chemosensitivity of EOC to paclitaxel is proposed.

## Materials and Methods

**Cell culture.** We used 11 human EOC cell lines. SKOV-3, NOS-2, TAOV, NOS-4, HRA, RMG-I, and RMG-II cells were cultured and maintained as described previously.[10,18,19] NOS-1 cells were established in our institute. ES-2, HEY, and KOC-7C cells were purchased from the American Type Culture Collection (ATCC; Manassas, VA, USA). Furthermore, acquired paclitaxel-resistant NOS-2 cells (NOS-PR cells) were established in our institute, as described previously.[20] These cell lines were maintained in RPMI-1640 (Sigma, St. Louis, MO, USA) supplemented with 10% fetal calf serum (FCS) and penicillin streptomycin at 37°C in a humidified atmosphere of 5% $CO_2$.

[1]To whom correspondence should be addressed.
E-mail: kajiyama@med.nagoya-u.ac.jp

doi: 10.1111/j.1349-7006.2009.01378.x

**Enzyme activity assay.** DPPIV enzyme activity was measured spectrophotometrically using Gly-Pro-p-nitroanilide-tosylate (Peptide Institute, Osaka, Japan) as a DPPIV substrate, as described previously.[10] We used diprotin A (DPA) (Peptide Institute) as a specific inhibitor of DPPIV enzyme activity.

**Generation of stable SKOV-3 clones expressing DPPIV.** Vector construction and generation of stable SKOV-3 clones expressing DPPIV were described previously.[10] Briefly, transfections were carried out using Lipofectamine according to the manufacturer's instructions (Invitrogen, San Diego, CA, USA). SKOV-3 cells were transfected with pcDNA3.1 (–), and pcDNA3.1 (–) with DPPIV cDNA was inserted. Stable transfectants were selected by growth in medium supplemented with 400 μg/mL of G418 (Sigma-Aldrich, St. Louis, MO, USA). Several hundred clones resistant to G418 were obtained. Since we hoped to eliminate any effects that could be attributed to clonal variation, polyclonal cells from these transfectants were used in the following experiments.[10]

**Flow cytometric analysis.** Fluorescence-activated cell sorting (FACS) was performed to quantify the expression levels of DPPIV on the cell surface of EOC cells. Then, the cells were incubated with phycoerythrin-conjugated monoclonal antibodies specific for DPPIV (Pharmingen, San Diego, CA, USA) for 30 min at 4°C, and washed three times with phosphate-buffered saline (PBS). FACS data were acquired using a FACS Calibur (Becton Dickinson, San Jose, CA, USA), and analyzed using CELL Quest software (Becton Dickinson).

**Cell proliferation assay.** SKpc and SKDP cells were plated in triplicate at a density of 1500 cells in a 100 μL volume in 96-well plates, and cultured for 1 to 4 or 5 days with/without 10% FCS, as described previously.[10] Cell viability was assayed using a modified tetrazolium salt MTT assay employing a CellTiter 96 AQueous One Solution Cell Proliferation Assay kit (Promega, Madison, WI, USA) according to the manufacturer's instructions. Absorbance was measured at 492 nm by a microplate reader (Multiskan Bichromatic; Labsystems, Helsinki, Finland).

**Paclitaxel chemosensitivity assay.** The paclitaxel chemosensitivity assay was performed as described previously.[21] Briefly, cells were seeded in triplicate in 96-well plates at a density of 5000 cells in a volume of 200 μL of culture media containing 10% FCS. After incubation for 24 h at 37°C, the medium was replaced with fresh medium with or without various concentrations of paclitaxel (Bristol Myers Squib, Tokyo, Japan). After an additional 72 h, cell viability was assayed using the Cell Titer 96 Aqueous One Solution Cell Proliferation Assay kit (Promega), as described above in 'Cell proliferation assay'. IC50 values indicate the concentrations resulting in a 50% reduction in growth as compared with control cell growth.

**Cell cycle analysis.** Cells were incubated in culture media alone or culture media and paclitaxel (70 ng/mL) at 37°C for 8 h. The cells were then collected, washed twice with PBS, and resuspended in PBS containing 10 μg/mL propidium iodide (PI), 0.5% Tween 20, and 0.1% RNase at room temperature for 30 min. Samples were then analyzed for their DNA content using a FACS Calibur (Becton Dickinson). Cell debris and fixation artifacts were gated out and G0/G1, S, and G2-M populations were quantified using CELL Quest software (Becton Dickinson).

**Western blot analysis.** Immunoblot analysis was performed as described previously.[22] Cells were seeded on 10-cm dishes in RPMI-1640 containing 10% FCS. After the cells reached subconfluency, the medium was replaced by fresh RPM-I1640 with or without paclitaxel (100 ng/mL). After 24 h of incubation, cell lysates were collected. Twenty μg of total cell lysate were electrophoresed on an SDS polyacryamide gel and transferred electrophoretically to Immobilon membranes (Millipore, Bedford, MA, USA). After blocking, the membrane was incubated for 1 h with the respective antihuman primary antibody at the recommended dilution (anti-DPPIV: Bender MedSystems, Vienna, Austria; anti-Apaf and Bcl-2: BD Transduction Laboratories, Franklin Lakes, NJ, USA; anti-Bcl-XL, Bad, and Bax: Cell Signaling, Danvers, MA, USA; TWIST, and β-actin: Santa Cruz Biotechnology, Santa Cruz, CA, USA). The primary antibodies were washed in Tween/PBS, and then incubated with horseradish peroxidase–conjugated secondary antibody. Proteins were visualized using enhanced chemiluminiscence (ECL) reagent (Amersham Biosciences, Tokyo, Japan), followed by exposure to X-ray film.

**Assay for apoptosis.** To quantify apoptosis, Annexin V and PI staining was performed, followed by FACS. Preparation of the cells and the assay for apoptosis was performed using the MEBCYTO apoptosis kit (MBL International, Woburn, MA, USA), as described previously.[21]

***In vivo* experiment.** A total of $2.0 \times 10^6$ SKpc and SKDP cells were subcutaneously inoculated in 0.2 mL of serum-free RPMI.1640 medium through a 24-gage needle into the lower flank of 5-week-old nude mice (Japan SLC, Nagoya, Japan). The subcutaneous tumor size was followed with or without the intraperitoneal (i.p.) administration of paclitaxel (20 mg/kg/body weight). To mice treated with paclitaxel, the i.p. injection of paclitaxel was initiated 20 days after tumor inoculation, and repeated twice a week for, at most, 6 weeks. Each group consisted of seven mice. The tumor was measured with calipers and the volume was calculated using the formula: $\pi/6 \times$ (largest diameter) $\times$ (smallest diameter)$^2$. Data are presented as the mean ± SD. Furthermore, apoptotic events after treatment with paclitaxel were determined by the TdT-mediated dUTP nick end-labeling (TUNEL) assay in xenograft tumor sections. Briefly, 4- μm paraffin-embedded tissue sections were prepared from the murine xenograft tumors. The slides were then subjected to TUNEL staining using an MEBSTAIN Apoptosis Kit according to the manufacturer's protocol (MBL International). The stained slides were analyzed using an BZ8000 (Keyence, Tokyo, Japan) fluorescence microscope. Apoptotic cells were identified by positive TUNEL staining. All procedures were performed in accordance with the regulations for animal experiments from the Division of Experimental Animals of Nagoya University, Japan.

**Statistical analysis.** For data from *in vitro* experiments, statistical comparisons among groups were performed using the Student's *t*-test. Differences between groups were considered significant at $P < 0.05$. Data are expressed as the mean ± SD. In addition, Spearman's correlation test was used to compare the IC50 values of paclitaxel and the mean fluorescence intensities of DPPIV among various EOC cell lines by FACS analysis. The time-course of tumor growth was compared across the treatment groups with the use of two-way ANOVA, with group and time as the variables.

## Results

**DPPIV/CD26 expression in EOC cell lines.** We first examined DPPIV expression in EOC cell lines by FACS analysis. DPPIV was generally expressed in cell lines, although the extent of its expression varied from cell to cell. The mean DPPIV fluorescence intensities of SKOV-3, ES-2, HRA, KOC-7C, and HEY cells were 12, 4, 4, 12, and 8, respectively. These EOC cell lines were negative or showed limited expressions of DPPIV. On the other hand, those of NOS-2, TAOV, NOS4, RMG-I, RMG-II, and NOS-1 cells were 684, 293, 292, 119, 167, and 746, respectively (Fig. 1A). These cell lines were positive for DPPIV expression, which is consistent with data obtained by enzyme activity analysis (Fig. 1B). We next examined the sensitivity to paclitaxel using these EOC cell lines. The IC50 values of SKOV-3, ES-2, HRA, KOC-7C, and HEY cells were 43.0, 41.2, 50.2, 28.1, and 41.8, respectively. In contrast, those of NOS-2, TAOV, NOS4, RMG-I, RMG-II, and NOS-1 cells were 6.9, 9.1,


doi: 10.1111/j.1349-7006.2009.01378.x

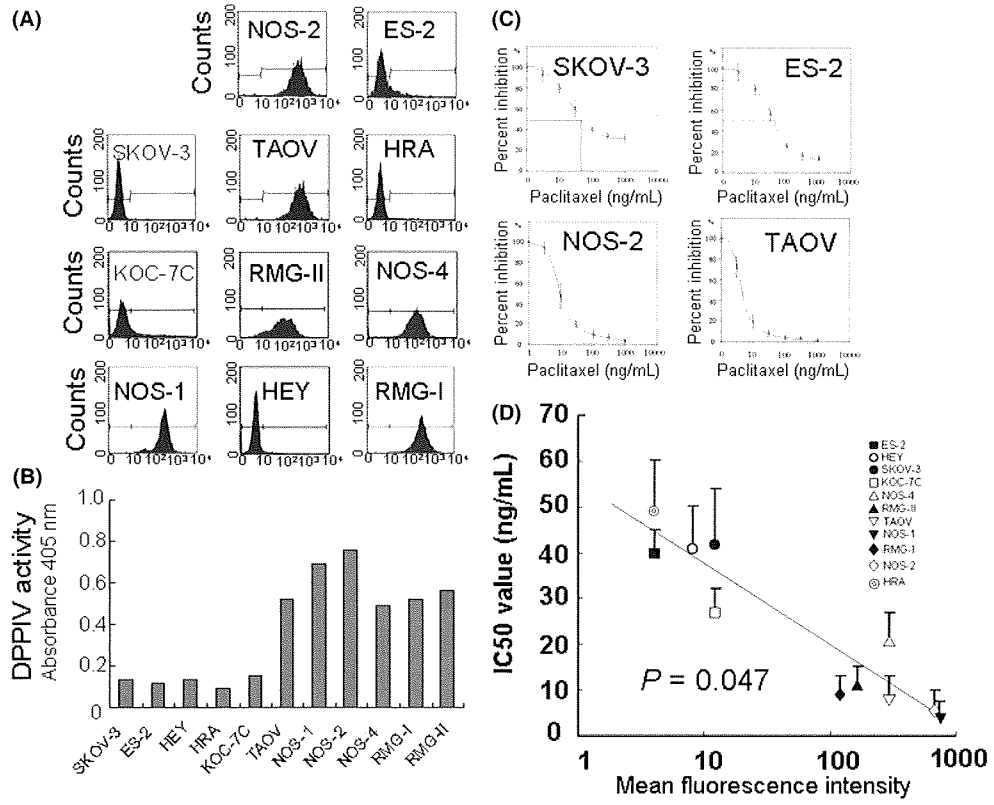


**Fig. 1.** The correlation between expressions of dipeptidyl peptidase IV (DPPIV) and sensitivity to paclitaxel in 11 epithelial ovarian cancer (EOC) cell lines. (A) The DPPIV expressions of 11 EOC cell lines are indicated as FACS data. The mean fluorescence intensities (MFIs) of DPPIV in the EOC cell lines SKOV-3, HEY, HRA, ES-2, KOC-7C, TAOV, NOS-1, NOS-2, NOS4, RMG-I, and RMG-II cells were 12, 8, 4, 4, 12, 293, 746, 684, 292, 119, and 167, respectively. (B) DPPIV activity of 11 EOC cell lines. DPPIV enzyme activity was measured at 405 nm after 45-min incubation at 37°C. (C) Sensitivity to paclitaxel of several representative EOC cell lines (SKOV-3, ES-2, NOS-2, and TAOV cells). IC50 values of these cell lines were 43.0, 41.2, 6.9, and 9.1, respectively. (D) The correlation between the MFI of DPPIV and IC50 value in 11 EOC cell lines. The IC50 values of these 11 cell lines were negatively correlated with DPPIV expression, as shown by the MFIs ($P = 0.047$, $r = -0.761$).

22.1, 10.5, 12.3, and 4.9, respectively. Representative data of SKOV-3, and ES-2, NOS2, and TAOV cells are shown in Figure 1(C). Figure 1(D) shows the correlation between the mean fluorescence intensity of DPPIV and IC50 values in 11 EOC cell lines. The results revealed that the expression of DPPIV and IC50 of paclitaxel were negatively correlated ($P = 0.0047$, $r = -0.761$).

**The effect of DPPIV overexpression on chemosensitivity to paclitaxel.** To investigate the effect of DPPIV transfection on chemosensitivity to paclitaxel in EOC cells, we overexpressed DPPIV in SKOV-3 cells (SKDP cells). While vector-transfected SKpc cells expressed little DPPIV on the cell surface, SKDPIV cells expressed a markedly high level of DPPIV using Western blot analysis (Fig. 2A). Figure 2(B) shows the paclitaxel sensitivity curve between SKDP and SKpc cells. The IC50 values of SKDP and SKpc cells were 6.2 and 40.0, respectively. The IC50 value of vector-transfected SKpc cells was almost the same as that of parental SKOV-3 cells. On the contrary, the transfection of DPPIV enhanced the sensitivity to paclitaxel up to the level of natively paclitaxel-sensitive EOC cells, such as NOS-2 or TAOV cells. To assess the effect of DPPIV on the *in vitro* proliferation potential, using these two lines, we performed growth assays on plastic dishes. As a result, we confirmed that the growth rates between these two lines were almost the same as each other on the plastic dishes (Fig. 2C). Subsequently, to investigate the mechanism of DPPIV-induced enhanced chemosensitivity, we assessed whether DPPIV transfection had an effect on paclitaxel-induced cell-cycle arrest in SKpc and SKDP cells. Cells were treated with paclitaxel (70 ng/mL) for 8 h, followed by PI staining and flow cytometric analysis. As shown in Figure 2(D), the enhancement of paclitaxel sensitivity observed in SKDP cells was attributable to an increase in the percentage of cells arresting at G2-M. Furthermore, to investigate the involvement of DPPIV activity, we assessed whether the inhibition of DPPIV activity using DPA influenced the paclitaxel sensitivity of either DPPIV-transfected SKDP cells or natively DPPIV-overexpressing NOS-2 cells. The DPPIV activity of SKDP cells was approximately 10-times higher than that of SKpc cells, and it was inhibited by adding 100 μM of DPA (Fig. 3A). Although DPA treatment did not alter the surface expression levels of DPPIV (Fig. 3B), the addition of DPA (100 μM) did not induce any apparent alteration of the sensitivity to paclitaxel in either SKDP or NOS-2 cells (Fig. 3C,D). According to this preliminary data, we did not identify a positive correlation between DPPIV activity and paclitaxel sensitivity in EOC cells.

**Effect of DPPIV transfection on paclitaxel-induced apoptosis of EOC cells.** We subsequently assessed whether the transfection of DPPIV had an effect on the paclitaxel-induced apoptosis of SKpc and SKDP cells. Cells were treated with paclitaxel (100 ng/mL) for 48 h, followed by Annexin V/PI staining and flow cytometric analysis. As shown in Figure 4(A), SKpc cells exhibited mild apoptosis on paclitaxel administration, while SKDP cells showed moderate to marked apoptosis. The quantitative data reveal that, compared to SKpc cells showing 6.2% apoptotic cells on paclitaxel treatment, SKDP cells showed a

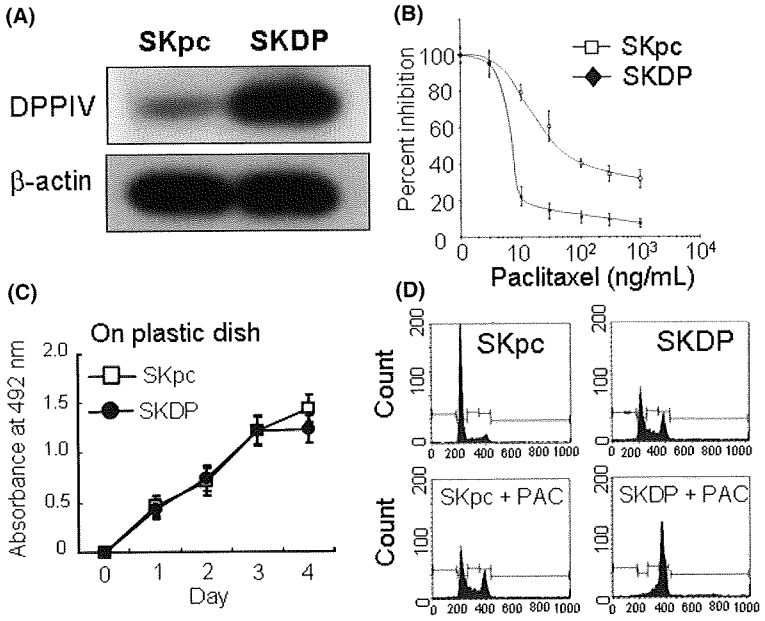


**Fig. 2.** The effect of dipeptidyl peptidase IV (DPPIV) overexpression on susceptibility to paclitaxel. (A) Enhanced expression of DPPIV in DPPIV-transfected cells. Western blot analysis using total cell lysates. (B) Transfection of DPPIV expression in SKOV-3 cells induced a marked increase in chemosensitivity to paclitaxel. The IC50 values of SKDP and SKpc cells were 6.2 and 40.0, respectively. (C) Effect of DPPIV transfection on cell proliferation on plastic dishes using SKDP and SKpc cells. Four-day proliferation curves of SKpc and SKDP cells in the presence of 10% FCS. Analysis of the proliferation rate was performed as described in the Materials and Methods. No significant differences between SKpc and SKDP cells were observed. Bars, SD. (D) Effect of DPPIV transfection on paclitaxel-mediated cell-cycle arrest at G2-M. SKpc and SKDP cells were incubated at 37°C in media containing paclitaxel (70 ng/mL) for 8 h. Data are representative of three separate experiments.

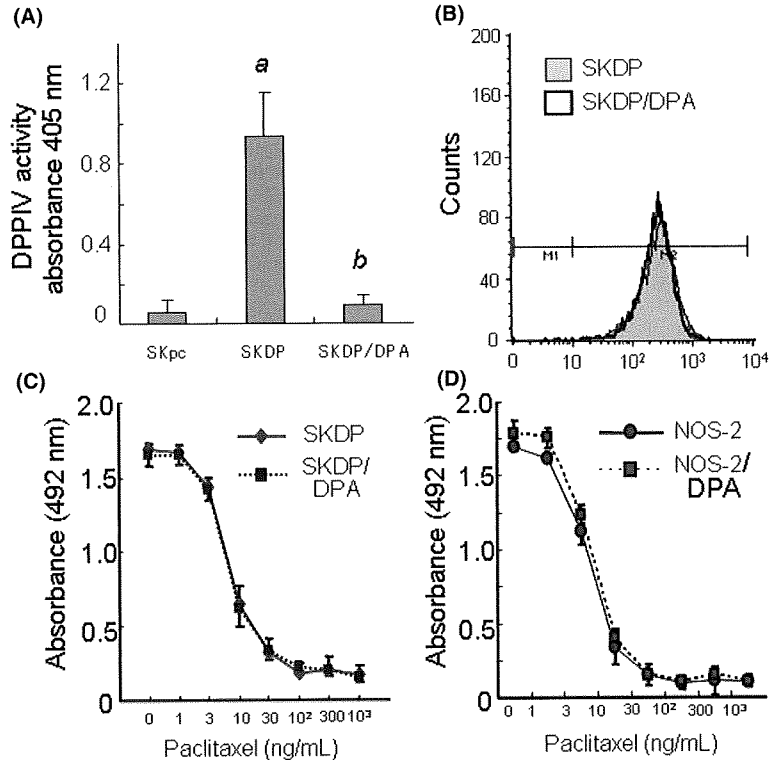


**Fig. 3.** The effect of a dipeptidyl peptidase IV (DPPIV) inhibitor (diprotin A, DPA) on chemosensitivity to paclitaxel in either DPPIV-transfected SKDP or natively DPPIV-overexpressing NOS-2 cells. (A) The DPPIV activity of SKDP cells with or without DPA (100 μM). (*a*) $P < 0.001$, SKpc *versus* SKDP cells; (*b*) $P < 0.001$, SKDP *versus* SKDP/DPA cells. (B) The surface expressions of DPPIV in the presence or absence of DPA (100 μM, 72 h). DPA-treatment did not alter the surface expression levels of DPPIV in SKDP cells. White peak, SKDP/DPA cells; gray peak, SKDP cells. (C) Inhibition of DPPIV activity by the addition of DPA (100 μM) in SKpc and SKDP cells. (D) Inhibition of DPPIV activity by the addition of DPA (100 μM) in NOS-2 cells.

marked increase in apoptosis, accounting for 19.1%. Subsequently, we examined whether the expressions of apoptosis markers varied in the presence or absence of treatment with paclitaxel using Western blot analysis. In the absence of paclitaxel, the expression levels of Bcl-2, Bcl-XL, Bax, and Bad were very similar between SKpc and SKDP cells. On the other hand, in the presence of paclitaxel, the expression levels of these proteins were markedly changed. Thus, the expression levels of Bcl-2 and Bcl-XL were decreased and those of Bax and Bad were increased in SKDP compared to SKpc cells (Fig. 4B). Furthermore, we examined whether the expression of TWIST, a master regulator of epithelial–mesenchymal transition (EMT), and possibly linked to paclitaxel resistance, was altered among these transfectants. Western blot analysis demonstrated that the down-regulated TWIST expression was observed in SKDP compared to that in SKpc cells. In addition, these tendencies were not altered on exposure to paclitaxel (Fig. 4C).

**The effect of serum starvation on the proliferation of SKpc and SKDP cells.** We subsequently hypothesized that if DPPIV overexpression led to an enhanced susceptibility to paclitaxel, it might be related to sensitivity to other cell stresses such as serum starvation. Figure 5(A) shows 5-day proliferation curves



doi: 10.1111/j.1349-7006.2009.01378.x

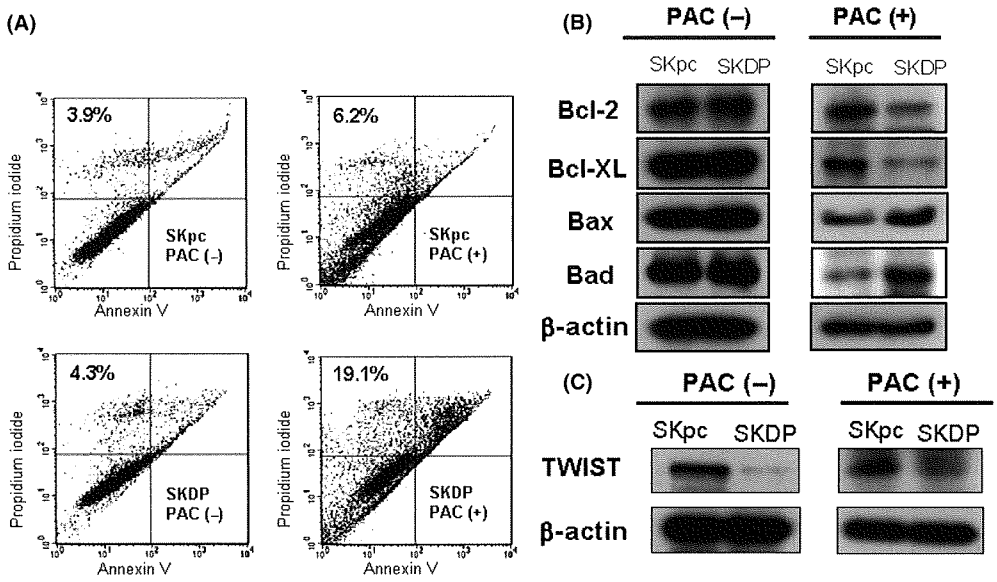


**Fig. 4.** Effect of dipeptidyl peptidase IV (DPPIV) transfection on the paclitaxel-induced apoptotic death of epithelial ovarian carcinoma (EOC) cells. (A) Detection of paclitaxel-induced apoptosis using Annexin V and propidium iodide (PI) assays of SKpc and SKDP cells treated with 100 ng/mL of paclitaxel for 48 h. The percentage of apoptotic cells calculated by flow cytometric analysis is presented. Each value (%) indicates Annexin V (+)/ PI (+) cells. (B) Change in expressions of apoptosis-related proteins with or without paclitaxel treatment using Western blot analysis. (C) Western blot analysis demonstrated down-regulated TWIST expression in SKDP compared to SKpc cells in the presence or absence of paclitaxel.

of SKpc and SKDP cells under serum-starved conditions. The proliferation rates were markedly lower in SKDP than in SKpc cells in serum-free media. SKpc cells were capable of growing even in serum-free media until 96 h after the beginning of starvation. In contrast, SKDP cells failed to proliferate in these media. Moreover, we examined whether the expression of apoptosis markers was affected under the serum-starved condition using Western blot analysis. The expression levels of Apaf, Bax, and Bad were upregulated in SKDP cells compared to those in SKpc cells after 96-h exposure to the serum-free condition. Furthermore, the expression level of BCl-2 was decreased (Fig. 5B).

**Downregulation of DPPIV expression and enzyme activity in EOC cells with acquired paclitaxel resistance.** We established and confirmed the resistance to paclitaxel of NOS-PR cells.[32] Figure 6(A) shows the paclitaxel-sensitivity assay of parental NOS-2 and resistant NOS-PR cells. More pronounced chemoresistance to paclitaxel was noted in NOS-PR compared to NOS-2 cells. The IC50 values of NOS-2 and NOS-PR cells were 9.3 and 367.3 ng/mL, respectively. The IC50 value of NOS-PR cells was considered to correspond to clinical paclitaxel resistance. We subsequently compared the surface expression levels of DPPIV between the NOS-PR and parental NOS-2 lines. With regard to the morphology, NOS-2 cells displayed an epithelioid and cobblestone appearance (Fig. 6B, left panel). In contrast, NOS-PR cells showed a loss of cell polarity, causing a spindle-shaped morphology, and the increased formation of pseudopodia (Fig. 6B, right panel). We already demonstrated that NOS-2 cells displayed a markedly high level of DPPIV, as shown in Figure 1(A). On the other hand, the DPPIV expression level of NOS-PR was lower than that of NOS-2 cells (Fig. 6C). Moreover, to confirm the enzyme activity of DPPIV protein, we also analyzed aminopeptidase activity. The DPPIV activity of NOS-PR cells was approximately one-sixth lower than that of parental NOS-2 cells in terms of absorbance (Fig. 6D). The DPPIV activities of both lines were almost completely inhibited by adding 100 μM of DPA. Furthermore, the inhibition of DPPIV activity using DPA did not influence either the cell morphology or paclitaxel sensitivity of both lines (data not shown).

**The effect of DPPIV overexpression on subcutaneous tumor formation in nude mice treated with paclitaxel.** Finally, we investigated whether DPPIV-sensitized tumors formed in nude mice receiving following subcutaneous xenografting. Subcutaneous tumor formation was observed at least approximately 1 week after the inoculation of mice with SKpc or SKDP cells. Subsequently, periodic i.p. treatment with PBS or paclitaxel was performed, as described in the Materials and Methods. Figure 7(A,B) shows the general appearance of mice treated with paclitaxel 39 or 61 days after inoculation with SKpc (left mouse) or SKDP cells (right mouse). Figure 7(C) shows the time-course of tumor-growth curves of both groups on paclitaxel treatment. Among the paclitaxel-treated mice, the subcuta-

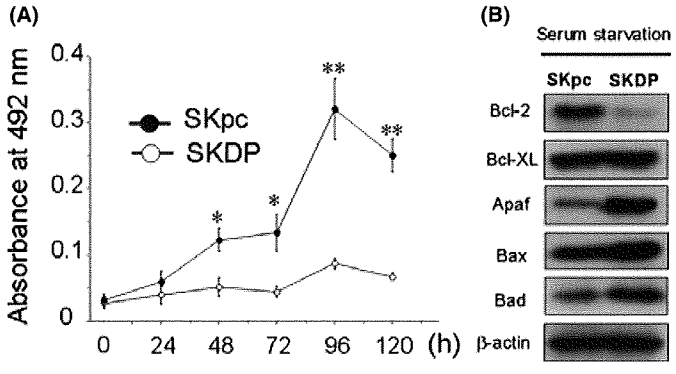


**Fig. 5.** The effect of serum starvation on the proliferation and expression levels of several apoptosis-related proteins in SKpc and SKDP cells. (A) Five-day proliferation curves of SKpc and SKDP cells under serum-starved conditions. Although SKpc cells were capable of growing even in serum-free media until 96 h after the beginning of starvation, SKDP cells failed to proliferate in these media. $*P < 0.001$; $**P < 0.0001$. (B) Change in the expression of apoptosis-related proteins under serum-starved conditions for 96 h using Western blot analysis.

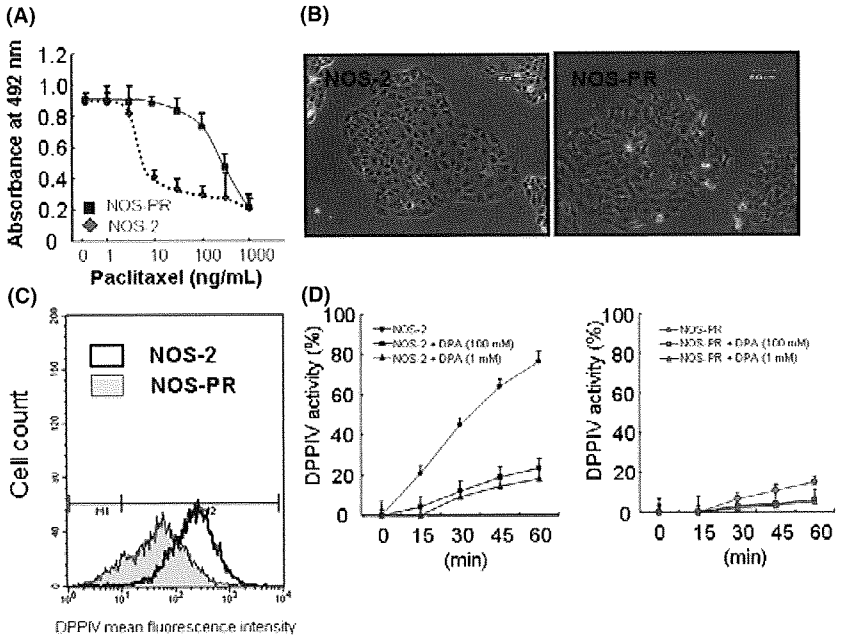


Fig. 6. Downregulation of dipeptidyl peptidase IV (DPPIV) expression and enzyme activity in epithelial ovarian carcinoma (EOC) cells with acquired paclitaxel resistance. (A) Paclitaxel sensitivity assay of parental NOS-2 and resistant NOS-PR cells. More pronounced chemoresistance to paclitaxel was noted in NOS-PR compared to NOS-2 cells. The IC50 values of NOS-2 and NOS-PR cells were 9.3 and 367.3 ng/mL, respectively. (B) The surface expression levels of DPPIV between the NOS-PR and parental NOS-2 lines. The expression level of DPPIV of NOS-PR cells was lower than that of NOS-2 cells. (C) Cell morphology of NOS-2 and NOS-PR cells. NOS-2 cells displayed an epithelioid and cobblestone appearance (left panel). NOS-PR cells showed the loss of cell polarity, leading to a spindle-shaped morphology (right panel). (D) The DPPIV activity of NOS-2 and NOS-PR cells. DPPIV activities of both lines were almost completely inhibited by the addition of 100 μM of DPA.

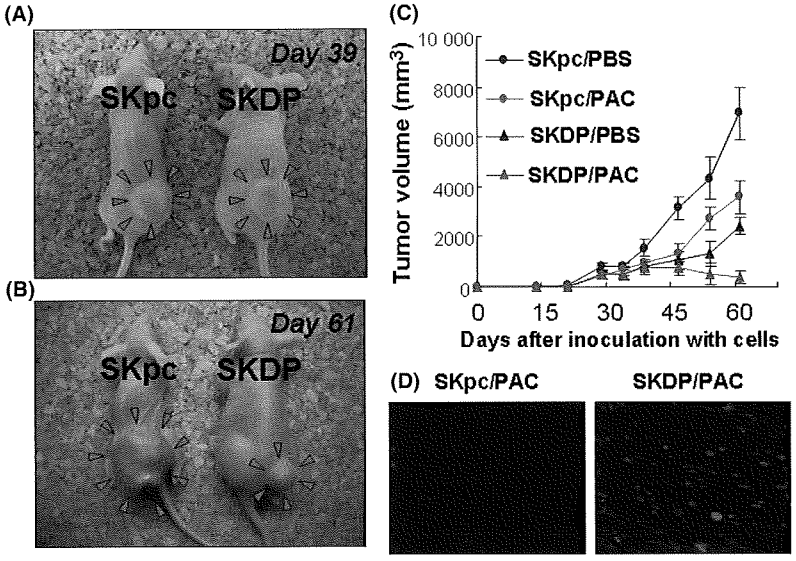


Fig. 7. The effect of the overexpression of dipeptidyl peptidase IV (DPPIV) on subcutaneous tumor formation in nude mice with or without treatment with paclitaxel. A total of $2.0 \times 10^6$ SKpc and SKDP cells were subcutaneously implanted in the lower flank of nude mice. Subsequent intraperitoneal (i.p.) administration of paclitaxel (20 mg/kg) or PBS was initiated 20 days after tumor inoculation, and repeated twice a week for a maximum of 6 weeks. (A,B) Among paclitaxel-treated mice, the general appearance of mice 39 (A) and 61 (B) days after inoculation with SKpc (left mouse) and SKDP (right mouse) cells. On Day 39, the tumor size of the SKDP cell-inoculated group was as large as that of the SKpc cell-inoculated group. In contrast, on Day 61, the former was smaller than the latter. (C) Tumor growth curves of the four groups: Red closed red circle (SKpc/PAC-group), SKpc-inoculated group treated with paclitaxel ($n = 7$); closed red triangle (SKDP/PAC-group), SKDP-inoculated group treated with paclitaxel ($n = 7$); closed blue circle (SKpc/PBS-group), SKpc-inoculated group treated with PBS ($n = 7$); closed blue triangle (SKDP/PBS-group), SKDP-inoculated group treated with PBS ($n = 7$). On Day 61: $P < 0.0001$, SKpc/PAC-group *versus* SKDP/PAC-group; $P < 0.0001$, SKpc/PBS-group *versus* SKDP/PBS-group. Data are presented as the mean ± SD. (D) TUNEL staining was performed for the resected murine subcutaneous tumor on Day 61. Apoptotic cells were identified by positive TUNEL staining (left panel, SKpc/PAC; right panel, SKDP/PAC).

neous tumor size following inoculation with SKDP cells was macroscopically almost the same as that in those inoculated with SKpc cells until 39 days after cell inoculation. In contrast, the difference between the sizes of both tumors increased from that time ($P < 0.0001$; Fig. 7C). This suggests that the enhancement of paclitaxel sensitivity *in vivo* might be in part due to the overexpression of DPPIV. Moreover, even in the absence of paclitaxel treatment, reduced *in vivo* tumor formation was observed in the SKDP cell-inoculated compared to the SKpc cell-inoculated group. Furthermore, TUNEL staining was performed for the resected murine subcutaneous tumor on Day 61. Positive TUNEL staining indicating apoptotic change was more clearly identified in the tumor formed by SKDP cells than that by SKpc cells (Fig. 7D).



doi: 10.1111/j.1349-7006.2009.01378.x

## Discussion

Paclitaxel exerts its effect through the stabilization of microtubules, induction of cell-cycle arrest in G2-M, and activation of proapoptotic signaling.[23,24] In the present study, we first showed that the surface expressions of DPPIV were positively correlated with sensitivities to paclitaxel in various EOC cell lines. This suggested that reduced DPPIV expression may be involved in the intrinsic resistance of EOC cells. Based on this observation, we subsequently demonstrated that the overexpression of DPPIV results in paclitaxel-induced apoptosis, and, consequently, promotes the susceptibility of EOC cells to paclitaxel. Thus far, Yamochi, *et al.* reported that in a B-cell lymphoma line, DPPIV expression was associated with the increased phosphorylation of p38 and its upstream regulators mitogen-activated protein kinase kinase 3/6 and apoptosis signal-regulating kinase 1, and that the p38 signaling pathway plays a role in the regulation of topoisomerase IIA expression, resulting in greater *in vitro* and *in vivo* tumor sensitivity to doxorubicin.[11] Regarding the link between DPPIV and chemosensitivity, their results were consistent with ours. However, to our knowledge, this is the first report showing a link between the expression of DPPIV and chemosensitivity to paclitaxel in solid tumors, especially EOC cells *in vitro* and *in vivo,* although the detailed mechanism remains under investigation.

Regarding the involvement of DPPIV enzyme activity in sensitivity to paclitaxel, the present data using DPPIV-transfected or natively DPPIV-overexpressing cells showed that sensitivity to paclitaxel did not change even on the simultaneous addition of a DPPIV inhibitor. DPPIV is a multifunctional molecule that has been reported to play an important role in cellular differentiation, signal transduction by tyrosine phosphorylation of a subset of small molecular mass proteins, and pathways, independent of its enzymatic activity.[25–28] Thus, regarding the link between DPPIV and sensitivity to paclitaxel, there may be a mechanism independent of DPPIV activity. We could not conclude that these data directly indicate the reduced involvement of DPPIV activity in the paclitaxel sensitivity of EOC, since a major limitation of this study was that we unfortunately did not perform an experiment using CD26-positive/DPPIV-negative mutants.

Considering the capability of DPPIV to cleave various selected biological factors, including neuropeptides, cytokines, and chemokines, which promote cancer metastasis, it is possible that DPPIV activity may contribute to antichemoresistance through proteolytically modifying peptides involved in anti-apoptotic signaling, and/or their precursors. Interestingly, our data demonstrated that under serum starvation DPPIV-transfected EOC cells did not proliferate with enhanced expressions of Apaf, Bax, and Bad; in contrast, vector-transfected cells did. This implies that DPPIV expression is involved in sensitivity to other cell stresses such as deficient growth factors, as well as exposure to paclitaxel. Wesley *et al.* showed that, in non-small-cell lung carcinoma cells, DPPIV induces cell cycle arrest and promotes the susceptibility of tumor cells to apoptosis upon serum withdrawal, and that both wild-type and mutant DPPIV in the enzyme activity region showing reduced levels of protease activity had similar effects on the induction of apoptosis.[29] Their data were consistent with ours, regardless of the involvement of DPPIV activity. However, if this result was due to increased DPPIV enzyme activity, the underlying mechanism may be based on serum withdrawal, possibly through the inactivation of some unidentified, essential growth factors involving DPPIV. For example, SDF-1α, a chemokine of the CXC subfamily, is a good substrate for DPPIV because it contains the preferred essential N-terminal X-Pro motif. Our earlier data demonstrated the involvement of the SDF-1α/CXCR4 axis in the enhanced peritoneal metastasis of EOC.[30] In glioma cells, SDF-1α prevented the apoptosis of tumor cells with the phosphorylation of Akt, a kinase associated with survival when serum is withdrawn from the culture medium, besides enhanced chemotaxis, in accordance with this better known role of chemokines.[31] Therefore, although the detailed mechanisms are still under investigation, at present, we think that DPPIV may be involved in signaling cascades regulating cell survival, protection from apoptosis, and paclitaxel resistance via both aminopeptidase-dependent and -independent mechanisms.

Generally, there are two types of resistance to antineoplastic agents: intrinsic and acquired chemoresistance. Clinically, recurrent EOC is frequently associated with acquired resistance to chemotherapeutic agents. In our earlier analysis, we established acquired paclitaxel-resistant EOC cell lines by their continuous exposure to increasing concentrations of paclitaxel.[32] Interestingly, in our current analysis, we further noted the decreased expression of DPPIV and activity in the acquired paclitaxel resistance of EOC cells compared to wild-type parental cells. Namely, the downregulation of DPPIV was observed accompanied by the gaining of paclitaxel resistance. Although, at present, we are unable to clearly explain its underlying mechanism and significance, we thought that there might be a possible relation between the decreased expression of DPPIV and not only intrinsic but also acquired chemoresistance. We plan to elucidate the role of DPPIV expression and its enzyme activity in refractory, recurrent EOC in the future.

Regarding the link between the morphologies of the above-mentioned EOC cell lines and paclitaxel sensitivity, weakly DPPIV-expressing cells were spindle-shaped, fibroblastic, and less paclitaxel-sensitive, while those of highly DPPIV-expressing EOC cells were epithelioid and had a cobblestone-like appearance, and were comparatively sensitive to paclitaxel. Recent reports have shown that there are close links between the expression of TWIST, a key regulator of EMT through the modulation of E-cadherin expression,[33] and lower chemosensitivity to paclitaxel.[34] In particular, Wang *et al.* demonstrated, through the analysis of eight nasopharyngeal carcinoma cell lines, that the upregulation of TWIST was associated with resistance to paclitaxel, and TWIST inactivation through small RNA interference led to an increased sensitivity to paclitaxel-induced cell death.[35] In our present results, DPPIV overexpression in EOC cells led to the downregulation of TWIST expression. Although they were very preliminary data, it is possible that the mechanism underlying DPPIV chemosensitivity is due to reduced TWIST expression, at least in part, regardless of aminopeptidase dependence. We plan to investigate the detailed correlation between DPPIV and TWIST in the next study.

In conclusion, the data obtained here suggest that DPPIV overexpression may lead to the reduced tumorigenicity and restoration of sensitivity to paclitaxel in EOC cells *in vitro* and *in vivo*. In addition, our finding that DPPIV expression may be an *in vivo* marker of tumor sensitivity to paclitaxel treatment may lead to future treatment strategies targeting DPPIV for selected human cancers in clinical practice.

## References


1 Fleischer B. CD26: a surface protease involved in T-cell activation. *Immunol Today* 1994; **15**: 180–4.
2 Heike M, Mobius U, Knuth A, Meuer S, Meyer zum Buschenfelde KH. Tissue distribution of the T cell activation antigen Ta1. Serological, immunohistochemical and biochemical investigations. *Clin Exp Immunol* 1988; **74**: 431–4.
3 Nemoto E, Sugawara S, Takada H, Shoji S, Horiuch H. Increase of CD26/dipeptidyl peptidase IV expression on human gingival fibroblasts upon stimulation with cytokines and bacterial components. *Infect Immun* 1999; **67**: 6225–33.
4 Mizutani S, Sumi S, Narita O, Tomoda Y. Purification and properties of human placental dipeptidyl peptidase IV. *Nippon Sanka Fujinka Gakkai Zasshi* 1985; **37**: 769–75.
5 Oravecz T, Pall M, Roderiquez G *et al.* Regulation of the receptor specificity and function of the chemokine RANTES (regulated on activation, normal T cell expressed and secreted) by dipeptidyl peptidase IV (CD26)-mediated cleavage. *J Exp Med* 1997; **186**: 1865–72.
6 Mentlein R. Dipeptidyl-peptidase IV (CD26) – role in the inactivation of regulatory peptides. *Regul Pept* 1999; **85** (1): 9–24.
7 Hanski C, Huhle T, Reutter W. Involvement of plasma membrane dipeptidyl peptidase IV in fibronectin-mediated adhesion of cells on collagen. *Biol Chem Hoppe Seyler* 1985; **366**: 1169–76.
8 Loster K, Zeilinger K, Schuppan D, Reutter W. The cysteine-rich region of dipeptidyl peptidase IV (CD 26) is the collagen-binding site. *Biochem Biophys Res Commun* 1995; **217**: 341–8.
9 Pethiyagoda CL, Welch DR, Fleming TP. Dipeptidyl peptidase IV (DPPIV) inhibits cellular invasion of melanoma cells. *Clin Exp Metastasis* 2000; **18**: 391–400.
10 Kajiyama H, Kikkawa F, Suzuki T, Shibata K, Ino K, Mizutani S. Prolonged survival and decreased invasive activity attributable to dipeptidyl peptidase IV overexpression in ovarian carcinoma. *Cancer Res* 2002; **62**: 2753–7.
11 Yamochi T, Aytac U, Sato T *et al.* Regulation of p38 phosphorylation and topoisomerase IIalpha expression in the B-cell lymphoma line Jiyoye by CD26/dipeptidyl peptidase IV is associated with enhanced in vitro and in vivo sensitivity to doxorubicin. *Cancer Res* 2005; **65**: 1973–83.
12 Wesley UV, McGroarty M, Homoyouni A. Dipeptidyl peptidase inhibits malignant phenotype of prostate cancer cells by blocking basic fibroblast growth factor signaling pathway. *Cancer Res* 2005; **65**: 1325–34.
13 Aytac U, Claret FX, Ho L *et al.* Expression of CD26 and its associated dipeptidyl peptidase IV enzyme activity enhances sensitivity to doxorubicin-induced cell cycle arrest at the G(2)/M checkpoint. *Cancer Res* 2001; **61**: 7204–10.
14 Sato K, Aytac U, Yamochi T *et al.* CD26/dipeptidyl peptidase IV enhances expression of topoisomerase II alpha and sensitivity to apoptosis induced by topoisomerase II inhibitors. *Br J Cancer* 2003; **89**: 1366–74.
15 Brun JL, Feyler A, Chene G, Saurel J, Brun G, Hocke C. Long-term results and prognostic factors in patients with epithelial ovarian cancer. *Gynecol Oncol* 2000; **78** (1): 21–7.
16 Taxman DJ, MacKeigan JP, Clements C, Bergstralh DT, Ting JP. Transcriptional profiling of targets for combination therapy of lung carcinoma with paclitaxel and mitogen-activated protein/extracellular signal-regulated kinase kinase inhibitor. *Cancer Res* 2003; **63**: 5095–104.
17 Lee JT Jr, Steelman LS, McCubrey JA. Phosphatidylinositol 3'-kinase activation leads to multidrug resistance protein-1 expression and subsequent chemoresistance in advanced prostate cancer cells. *Cancer Res* 2004; **64**: 8397–404.
18 Kajiyama H, Shibata K, Terauchi M *et al.* Neutral endopeptidase 24.11/CD10 suppresses progressive potential in ovarian carcinoma in vitro and in vivo. *Clin Cancer Res* 2005; **11**: 1798–808.
19 Kajiyama H, Kikkawa F, Khin E, Shibata K, Ino K, Mizutani S. Dipeptidyl peptidase IV overexpression induces up-regulation of E-cadherin and tissue inhibitors of matrix metalloproteinases, resulting in decreased invasive potential in ovarian carcinoma cells. *Cancer Res* 2003; **63**: 2278–83.
20 Umezu T, Kajiyama H, Terauchi M *et al.* Establishment of a new cell line of endometrioid carcinoma of the ovary and its chemosensitivity. *Hum Cell* 2007; **20**: 71–6.
21 Yamashita M, Kajiyama H, Terauchi M *et al.* Involvement of aminopeptidase N in enhanced chemosensitivity to paclitaxel in ovarian carcinoma in vitro and in vivo. *Int J Cancer* 2007; **120**: 2243–50.
22 Shibata K, Kikkawa F, Nawa A, Suganuma N, Hamaguchi M. Fibronectin secretion from human peritoneal tissue induces Mr 92,000 type IV collagenase expression and invasion in ovarian cancer cell lines. *Cancer Res* 1997; **57**: 5416–20.
23 Horwitz SB. Taxol (paclitaxel): mechanisms of action. *Ann Oncol* 1994; **5** (Suppl 6): S3–6.
24 Wang TH, Wang HS, Soong YK. Paclitaxel-induced cell death: where the cell cycle and apoptosis come together. *Cancer* 2000; **88**: 2619–28.
25 Wesley UV, Albino AP, Tiwari S, Houghton AN. A role for dipeptidyl peptidase IV in suppressing the malignant phenotype of melanocytic cells. *J Exp Med* 1999; **190**: 311–22.
26 Sedo A, Malik R, Krepela E. Dipeptidyl peptidase IV in C6 rat glioma cell line differentiation. *Biol Chem* 1998; **379** (1): 39–44.
27 Sedo A, Kraml J. Dipeptidyl peptidase IV in cell proliferation and differentiation. *Sb Lek* 1994; **95**: 285–8.
28 Iwata S, Morimoto C. CD26/dipeptidyl peptidase IV in context. The different roles of a multifunctional ectoenzyme in malignant transformation. *J Exp Med* 1999; **190**: 301–6.
29 Wesley UV, Tiwari S, Houghton AN. Role for dipeptidyl peptidase IV in tumor suppression of human non small cell lung carcinoma cells. *Int J Cancer* 2004; **109**: 855–66.
30 Kajiyama H, Shibata K, Terauchi M, Ino K, Nawa A, Kikkawa F. Involvement of SDF-1alpha/CXCR4 axis in the enhanced peritoneal metastasis of epithelial ovarian carcinoma. *Int J Cancer* 2008; **122** (1): 91–9.
31 Zhou Y, Larsen PH, Hao C, Yong VW. CXCR4 is a major chemokine receptor on glioma cells and mediates their survival. *J Biol Chem* 2002; **277**: 49481–7.
32 Kajiyama H, Shibata K, Terauchi M *et al.* Chemoresistance to paclitaxel induces epithelial-mesenchymal transition and enhances metastatic potential for epithelial ovarian carcinoma cells. *Int J Oncol* 2007; **31**: 277–83.
33 Comijn J, Berx G, Vermassen P *et al.* The two-handed E box binding zinc finger protein SIP1 downregulates E-cadherin and induces invasion. *Mol Cell* 2001; **7**: 1267–78.
34 Zhang X, Wang Q, Ling MT, Wong YC, Leung SC, Wang X. Anti-apoptotic role of TWIST and its association with Akt pathway in mediating taxol resistance in nasopharyngeal carcinoma cells. *Int J Cancer* 2007; **120**: 1891–8.
35 Wang X, Ling MT, Guan XY *et al.* Identification of a novel function of TWIST, a bHLH protein, in the development of acquired taxol resistance in human cancer cells. *Oncogene* 2004; **23**: 474–82.




doi: 10.1111/j.1349-7006.2009.01378.x

Cancer Science
The official journal of the Japanese Cancer Association JCA

# Gene silencing of glypican-3 in clear cell carcinoma of the ovary renders it more sensitive to the apoptotic agent paclitaxel *in vitro* and *in vivo*

Tomokazu Umezu,[1] Kiyosumi Shibata,[1,3] Maiko Shimaoka,[1] Hiroaki Kajiyama,[1] Eiko Yamamoto,[1] Kazuhiko Ino,[1] Akihiro Nawa,[1] Takeshi Senga[2] and Fumitaka Kikkawa[1]

[1]Department of Obstetrics and Gynecology, Nagoya University Graduate School of Medicine, Showa-ku, Nagoya; [2]Division of Cancer Biology, Nagoya University Graduate School of Medicine, Showa-ku, Nagoya, Japan

(Received July 15, 2009/Revised September 10, 2009/Accepted September 10, 2009/Online publication October 27, 2009)

**Glypican-3 (GPC3) is a heparan sulfate proteoglycan that is bound to the cell membrane by a glycosylphosphatidylinositol (GPI) anchor, and glypicans can regulate the activity of a wide variety of growth and survival factors. We report here that GPC3 was expressed in clear cell carcinoma of the ovary, and not in other carcinomas. To evaluate the phenotype and potential preclinical relevance, we generated an ovarian cancer cell line stably transfected with plasmids encompassing shRNA targeting GPC3. We show that the clear cell carcinoma cell line with silenced GPC3 expression (GPC3 [–]) was more sensitive to paclitaxel than GPC3 (+) cells. In addition, the GPC3 silencing induced sensitization to paclitaxel was associated with the activation of an apoptosis pathway, as shown by flow cytometry. Moreover, we investigated the effect of GPC3 on peritoneal metastases using nude mice. Peritoneal metastases caused by GPC3 (–) were more sensitive to paclitaxel than those caused by GPC3 (+) cells. These results indicate that increased GPC3 expression in a clear cell carcinoma cell line may play a protective role against apoptosis, and so the downregulation of GPC3 may be a potential target to increase sensitivity to paclitaxel-induced apoptosis in clear cell carcinoma. (*Cancer Sci* 2010; 101: 143–148)**

Over the last two decades, aggressive cytoreductive surgery and chemotherapy have been used in an attempt to improve the survival rate in patients with EOC.[1–3] However, the long-term survival rate remains poor as a result of recurrence and the emergence of drug resistance. Based on morphological criteria, there are four major types of primary epithelial adenocarcinoma, and the chemosensitivity and biologic behaviors differ among these histologic types. Although ovarian carcinoma cells are generally sensitive to anticancer drugs, CCC is resistant to most of these agents. Thus, the prognosis for CCC patients is poor compared to other types of EOC such as serous adenocarcinoma.[4,5] CCC comprises more than 15% of EOC cases in Japan, although it represents 8–10% of all EOC cases in the USA.[5,6] Therefore, it is important to establish new treatment strategies to improve the prognosis of CCC patients.

Glypicans are a family of heparan sulfate proteoglycans that are linked to the exocytoplasmic surface of the plasma membrane through a glycosylphosphatidylinositol anchor. Six glypicans have been identified in mammals (GPC1–GPC6), and two in *Drosophila*.[7] The physiological function of glypicans is still not well understood. However, it was shown that the GPC3-encoding gene is mutated in patients with Simpson–Golabi–Behmel syndrome, an X-linked disorder characterized by pre- and postnatal overgrowth and a varying range of dysmorphisms.[7] GPC3 regulates cell growth either positively or negatively depending on the cell type. Genetic and functional studies showed that glypicans regulate the signaling activity of various morphogens, including Wnts, Hedgehogs, bone morphogenic proteins, and fibroblast growth factors.[8–12] Previous studies showed that GPC3 was overexpressed in Wilms' tumor, hepatocellular carcinoma, and hepatoblastoma.[13,14] In ovarian carcinoma, GPC3 was overexpressed in yolk sac tumor and CCC.[15–17] However, GPC3 function in CCC was unclear.

In the present study, we examined the phenotype and preclinical relevance of the downregulation of GPC3 *in vitro* and *in vivo* by using an RNA interference system comprising a stably integrated cassette for the expression of shRNA targeting GPC3.

Furthermore, we investigated the role of this molecule in the sensitivity of CCC to paclitaxel, which is a key drug for ovarian cancer, using shRNA targeting GPC3.

## Materials and Methods

**Cell culture.** We used eight human ovarian carcinoma cell lines (SKOV-3, HEY, ES-2, OVCAR-3, HRA, RMG-I, RMG-II, and KOC-7c) in this study. SKOV-3, HRA, RMG-I, and RMG-II cells were cultured and maintained as described previously.[18,19] ES-2, HEY, and KOC-7c cells were purchased from the American Type Culture Collection (Manassas, VA, USA). The cell lines were maintained in RPMI-1640 supplemented with 10% FCS and penicillin–streptomycin at 37°C in a humidified atmosphere of 5% $CO_2$.

**Sensitivity to paclitaxel.** The sensitivity of the cells to paclitaxel was determined using a modified tetrazolium salt MTS assay using the CellTiter 96 Aqueous One Solution Cell Proliferation Assay kit (Promega, Madison, WI, USA). Briefly, cells were trypsinized and plated out at a density of 5000 cells per well into 96-well plates. The cells were cultured overnight then given fresh medium containing various concentrations of paclitaxel. After incubation for 72 h, cell viability was assayed, and the cytotoxity was expressed as the $IC_{50}$ for each of the cell lines; that is, the concentration of the drug that caused a 50% reduction in absorbance at 490 nm relative to untreated cells.

**Glypican-3 shRNA and its transfection.** Short hairpin RNA was designed by us and synthesized by Qiagen-Xeragon (Germantown, MD, USA) to target GPC3: CCAATGCCATGTTCAAGAATTCAAGAGATTCTTGAACATGGCATTGGTTTTT and its antisense oligonucleotide. The scrambled shRNA (Qiagen-Xeragon) was used as a control. The oligonucleotides were annealed and inserted into RNAi-Ready pSIREN-RetroQ-TetP vector (Takara Bio, Tokyo, Japan). To establish a stable cell line, the vector plasmid was transfected into parental KOC-7c

[3]To whom correspondence should be addressed.
E-mail: shiba@med.nagoya-u.ac.jp

doi: 10.1111/j.1349-7006.2009.01382.x

cells using Lipofectamine 2000 reagent (Invitrogen, San Diego, CA, USA) and selected by adding puromycin.

**Western blot analysis.** Cell lysates were electrophoresed in SDS polyacrylamide gels under reducing conditions. After electrophoresis, the proteins were transferred electrophoretically to an Immobilon membrane (Millipore, Bedford, MA, USA). After blocking, the membrane was incubated for 1 h with the relevant antihuman primary antibody at the recommended dilution, GPC3 (BioMosaics, Burlington, VT, USA), cleaved-PRAP (Cell Signaling Technology, Danvers, MA, USA), and β-actin (Abcam, Cambridge, MA, USA). The membrane was washed three times with Tween/PBS for 15 min, then incubated with the appropriate secondary antibody for 1 h. After washing with Tween/PBS, the membrane was treated with ECL-Western blotting detecting reagent (Amersham Biosciences KK, Tokyo, Japan).

**Proliferation assay.** To study the effect of silencing GPC3 on KOC-7c cell growth, $5 \times 10^3$ KOC-7c cells per well were seeded in 96-well plates in culture medium supplemented with 10% FCS, and transfected with GPC3 shRNA or control shRNA. Following overnight incubation, the culture medium was replaced with fresh complete medium containing 10% FCS. After 24, 48, and 72 h, cell proliferation was assessed as previously described.[22]

***In vitro* cell migration assay.** The cell migratory potential was evaluated using 24-well Transwell chambers with 8.0 μm pore membranes (Corning, Corning, NY, USA). Cells were suspended in the upper chamber at a density of $5 \times 10^4$ in 200 μL serum-free medium. The lower chamber contained 800 μL medium supplemented with 10% FCS as a chemoattractant. After incubation for 16 h, the remaining cells on the upper surface of the filters were removed by wiping with cotton swabs, and migrating cells on the lower surface were stained using May-Grunwald Giemsa. The number of cells on the lower surface of the filters was counted under a microscope. Data were obtained from three individual experiments in triplicate.

**Assay for apoptosis.** To quantify the apoptosis of KOC-7c cells, annexin V and PI staining was carried out, followed by flow cytometry. Cells were briefly plated at a density of $1 \times 10^6$ per well into 10 cm dishes and treated with paclitaxel for 24 h. After treatment, both floating and attached cells were collected by brief trypsinization and washed with PBS twice, then subjected to annexin V and PI staining using a MEBCYTO apoptosis kit (MBL International, Woburn, MA, USA). After staining, quantitative analysis for apoptosis was carried out by flow cytometry.

**TUNEL assay.** The TUNEL assay (Apoptosis *in situ* Detection Kit; Wako Pure Chemical, Osaka, Japan) was used to detect apoptotic cell death by the enzymatic labeling of DNA strand breaks with fluorescein-deoxyuridine triphosphate and terminal deoxynucleotidyl transferase.

***In vivo* studies.** Female nude mice (BALB/c) at 5 weeks of age were obtained from Japan SLC (Nagoya, Japan). The treatment protocol followed the guidelines for animal experimentation adopted by Nagoya University (Nagoya, Japan). Control and sh GPC3 cells ($1 \times 10^7$ cells per 0.5 mL of medium/mouse) were injected i.p. to generate peritoneal metastasis of ovarian carcinoma in the mouse model. The i.p. injection of paclitaxel (20 mg/kg body weight) was initiated 48 h after tumor inoculation, and was repeated twice.

**Statistical analysis.** For data from *in vitro* experiments, statistical comparisons among groups were carried out using Student's *t*-test. Differences between groups were considered significant at $P < 0.05$.

## Results

**Glypican-3 expression and the $IC_{50}$ value of paclitaxel in EOC cell lines.** We evaluated GPC3 expression in EOC cell lines by Western blot (Fig. 1A). Only KOC-7c cells were strongly positive for GPC3 expression. In contrast, no serous carcinoma cell lines showed the expression of GPC3. We evaluated the $IC_{50}$ value of paclitaxel in EOC cell lines. KOC-7c was the most resistant to paclitaxel in CCC cell lines. However, some serous adenocarcinoma cell lines were more resistant to paclitaxel than KOC-7c (Table 1).

**Short hairpin RNA-mediated inhibition of GPC3 expression.** Previously, we used siRNAs targeting GPC3 to knock down endogenous gene expression. However, the major disadvantage of this strategy is the short duration of the silencing effect. In order to study the function of GPC3 in long-term growth *in vitro* and *in vivo*, we used an shRNA technique targeting GPC3. Control shRNA was also prepared. Each construct produced shRNA composed of two 21-nucleotides with an inverted orientation. GPC3 shRNA and control shRNA were used to transfect KOC-7c cells. The cells were further cultured in selective medium. After 6 weeks, the cell clones were selected and seeded for further expansion in selective medium for Western blot analysis. The protein level of GPC3 shRNA cells was almost zero, compared to that of GPC3 in control shRNA and parent cells. In contrast to GPC3, β-actin was not affected (Fig. 1B).

**Effect of GPC3 knockdown on *in vitro* cell proliferation and migration.** There was no significant difference in cell proliferation between control and sh GPC3 cells (Fig. 2A). Similarly, the silencing of GPC3 did not affect the migratory potential (Fig. 2B).

**Effect of GPC3 knockdown on *in vitro* paclitaxel sensitivity.** Previous studies suggested that GPC3 might be involved in chemoresistance to anticancer agents in gastric carcinoma cell lines.[20] Thus, we subsequently evaluated chemosensitivity on the GPC3 silencing of KOC-7c cells *in vitro*. We observed that

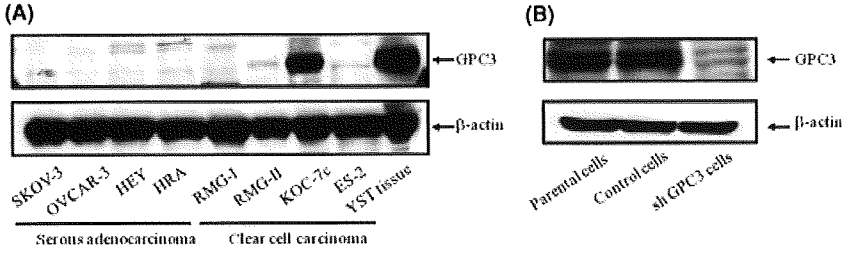


**Fig. 1.** (A) Glypican-3 (GPC3) expression in various epithelial ovarian cancer cell lines. YST, yolk sac tumor. (B) Effect of the suppression of GPC3 expression by sh RNA in KOC-7c ovarian cancer cells.

**Table 1. $IC_{50}$ values of various epithelial ovarian carcinoma cell lines**

| SKOV-3 | OVCAR-3 | HEY | HRA | RMG-I | RMG-II | KOC-7c | ES-2 |
|---|---|---|---|---|---|---|---|
| 16 ± 3.4 | 6.8 ± 1.8 | 7.4 ± 1.0 | 69.6 ± 10.2 | 4.8 ± 1.2 | 4.3 ± 1.1 | 15.4 ± 2.6 | 11.3 ± 2.2 |



doi: 10.1111/j.1349-7006.2009.01382.x

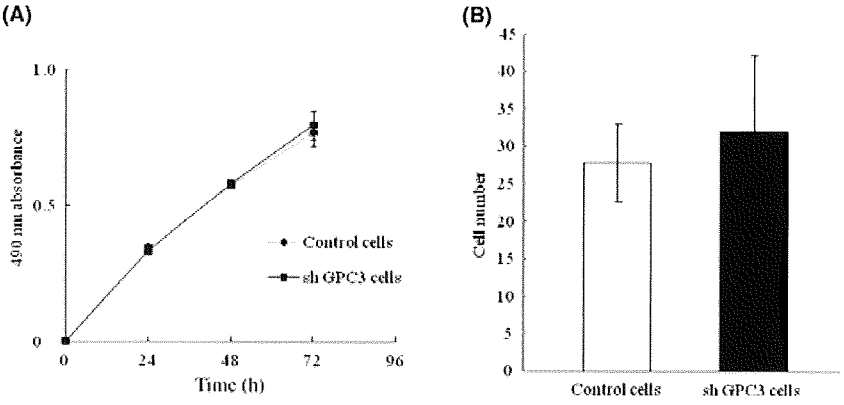


**Fig. 2.** (A) *In vitro* proliferation assay to assess the effect of silencing glypican-3 (sh GPC3) on growth of KOC-7c ovarian cancer cells. (B) *In vitro* cell migration assay to evaluate the potential of KOC-7c cells to migrate into Transwell chambers. The silencing of GPC3 did not affect the cells' migratory potential.

sh GPC3 cells were more sensitive to paclitaxel than control cells. The $IC_{50}$ value for paclitaxel of sh GPC3 cells was 4.5 ± 1.6 ng/mL. In contrast, that in control cells was 9.5 ± 1.5 ng/mL (Table 2). Cell death with morphological changes associated with apoptosis was more frequently observed in sh GPC3 cells (Fig. 3A–D).

**Effect of GPC3 knockdown on paclitaxel-induced apoptotic death of KOC-7c cells.** To further investigate the mechanism of GPC3 silencing-induced chemosensitivity, we also assessed the paclitaxel-induced apoptosis of control and sh GPC3 cells using flow cytometry. Cells were treated with paclitaxel (10 ng/mL) for 8 h, then subjected to annexin V/PI staining and flow cytometric analysis. As shown in Figure 3(E,F), sh GPC3 cells treated with paclitaxel showed a stronger apoptotic effect than control cells. The quantitative data showed that, compared to control cells treated with paclitaxel (10.8 ± 1.6% apoptotic cells), paclitaxel-treated sh GPC3 cells showed a significant increase in apoptosis (37.0 ± 3.9% apoptotic cells) (Fig. 3G). We measured cleaved PARP in control and sh GPC3 cells after exposure to paclitaxel by Western blot analysis. As shown in Figure 3(H), cleaved PARP expression in sh GPC3 cells showed an increase at 3 h after treatment with 10 ng/mL paclitaxel.

**Effect of GPC3 knockdown on peritoneal progression in nude mice.** To determine the role of GPC3 in peritoneal progression, the peritoneal progression of control and sh GPC3 cells was evaluated in a nude mouse model. Carcinomatous peritonitis was observed for 3 weeks after the inoculation of mice with $1 \times 10^7$ control and sh GPC3 cells. As shown in Figure 4A,B, the progression rate of peritoneal dissemination in sh GPC3 cells-inoculated was not significantly different from that in control cell-inoculated. The total cell-inoculated mice tumor volume was not different between control and sh GPC3 cells ($P = 0.67$) (Fig. 4C). Histologic findings confirmed that xenografted tumors of sh GPC3 cells showed attenuated GPC3 expression (Fig. 4D,E).

**Effect of GPC3 knockdown on *in vivo* paclitaxel sensitivity.** We tested whether GPC3 influenced CCC sensitivity to paclitaxel in a model using nude mice. Two days after inoculation of the mouse peritoneum with $1 \times 10^7$ control and sh GPC3 cells, 20 mg/kg body weight of paclitaxel was given once a week, a total of three times. Twenty-one days after the final treatment with paclitaxel, mice were dissected. The control cell group showed more disseminated tumors and a larger amount of bloody ascites compared with the sh GPC3 cell group (Fig. 5A,B). The total tumor volume in the mouse peritoneum in the presence of control cells was relatively large, compared to that in the presence of sh GPC3 cells ($P = 0.09$) (Fig. 5C). Finally, we used the TUNEL method to visualize DNA fragmentation at the single-cell level (Fig. 5D,E). After paclitaxel treatment, more apoptotic cells were observed in the sh GPC3 cell xenograft group than in the control cell group after paclitaxel treatment, although this was not significant ($P = 0.42$) (Fig. 5F).

**Table 2. Effect of shRNA on the sensitivity of KOC-7c ovarian cancer cells to paclitaxel**

| | Mean $IC_{50}$ ± SEM Paclitaxel (ng/mL) |
|---|---|
| Control shRNA | 9.5 ± 1.5 |
| Glypican-3 shRNA | 4.5 ± 1.6 |

## Discussion

Clear cell carcinoma has been classified as a subgroup of EOC and reported to be an interesting histologic type with unique clinical features. CCC showed a poorer prognosis compared to serous adenocarcinoma because it tended to be resistant to antineoplastic agents, including paclitaxel.[4,5] Paclitaxel is a first-line chemotherapeutic agent that is effective for the treatment of ovarian carcinoma. Paclitaxel exerts its effect through the stabilization of microtubules, induction of cell cycle arrest in $G_2$-M, and activation of pro-apoptotic signaling. However, in spite of the comparatively high sensitivity of ovarian carcinoma to paclitaxel, the prognosis of CCC patients remains poor as most deaths are the result of metastasis that is refractory to conventional chemotherapy. To overcome the paclitaxel resistance of CCC, a variety of additional molecular targeting therapies combined with paclitaxel have been investigated. The mechanisms of paclitaxel resistance have previously been explained by *MDR-1*/P-glycoprotein overexpression, and the selective expression of β-tubulin isotypes. Overexpression of the *MDR-1* gene, encoding an efflux pump (P-glycoprotein), leads to the efflux of paclitaxel and other cationic drugs, thereby hampering drug retention.[21]

Such a mechanism is easily observable in *in vitro*-cultured cancer cells. However, in the present analysis, there was no difference in *MDR-1* expression between control and sh GPC3 cells (data not shown). Class III β-tubulin seems to enhance dynamic instability, thereby overcoming the suppression of microtubule dynamicity by paclitaxel.[22] Thus, we evaluated class III β-tubulin expression in control and sh GPC3 cells. The results showed that there were no differences in class III β-tubulin between control and sh GPC3 cells (data not shown).

A previous report showed that 60% of ovarian CCC cases expressed GPC3. Our data also showed that 40% of CCC cases expressed GPC3. However, the function of GPC3 in CCC remains unclear. One reason for this might be the lack of a stable knockdown of GPC3 in human cancer cell lines available for both *in vitro* and *in vivo* experiments. In this study, we were the

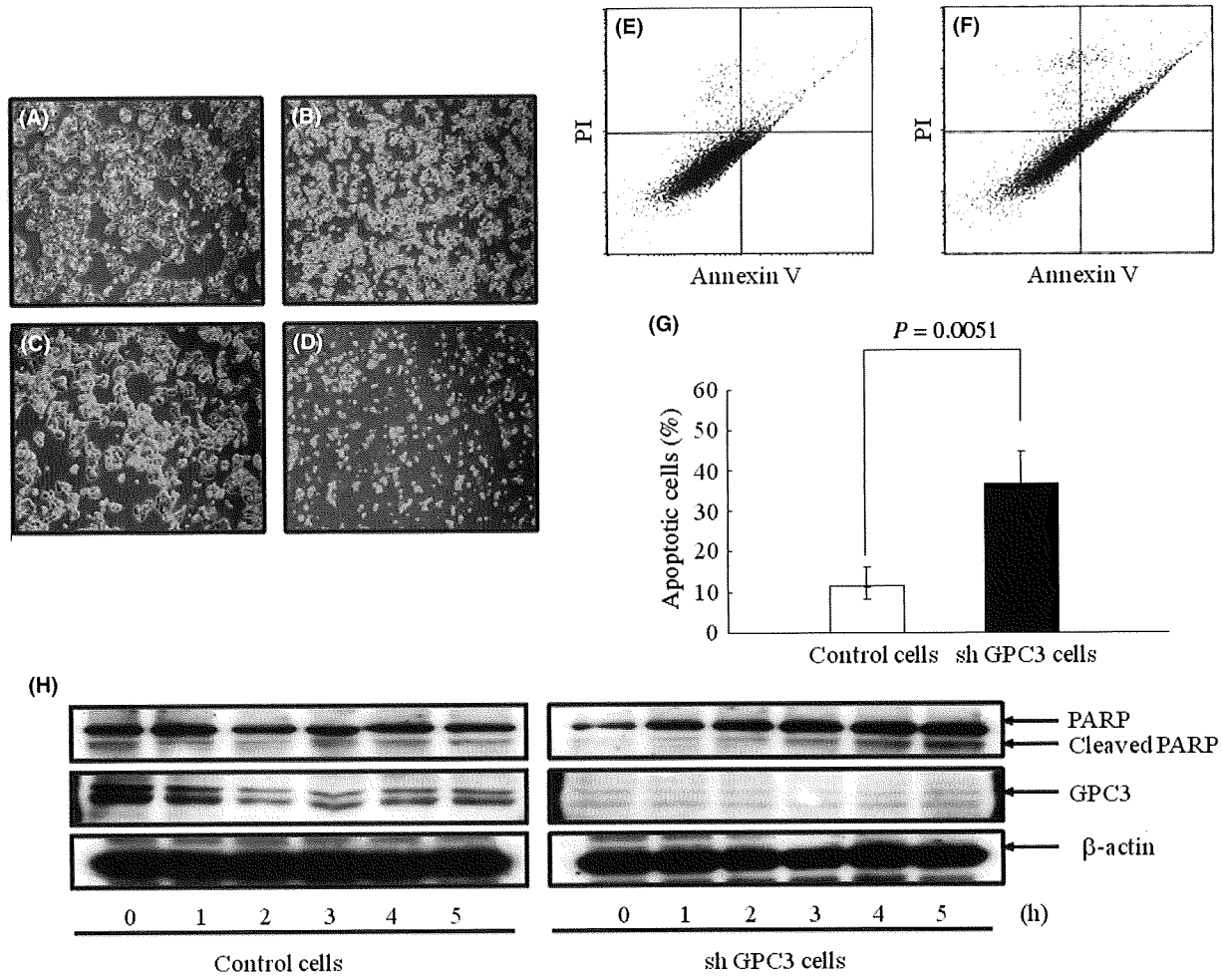


**Fig. 3.** (A–D) Morphological changes in control cells and clear cell carcinoma cells with silenced glypican-3 expression (sh GPC3) incubated with paclitaxel (10 ng/mL). (A) Control cells treated with paclitaxel for 24 h. (B) sh GPC3 cells treated with paclitaxel for 24 h. (C) Control cells treated with paclitaxel for 48 h. (D) sh GPC3 cells treated with paclitaxel for 48 h. (E–H) Effect of paclitaxel on the apoptosis of control and sh GPC3 cells. Cells were incubated with paclitaxel (10 ng/mL) for 8 h. The cells were then harvested, stained with annexin V/propidium iodide (PI), and analyzed by flow cytometry. (E) Control cells. (F) sh GPC3 cells. (G) Percentage of apoptotic cells. (H) Expression level of cleaved PARP, GPC3, and β-actin after paclitaxel treatment.

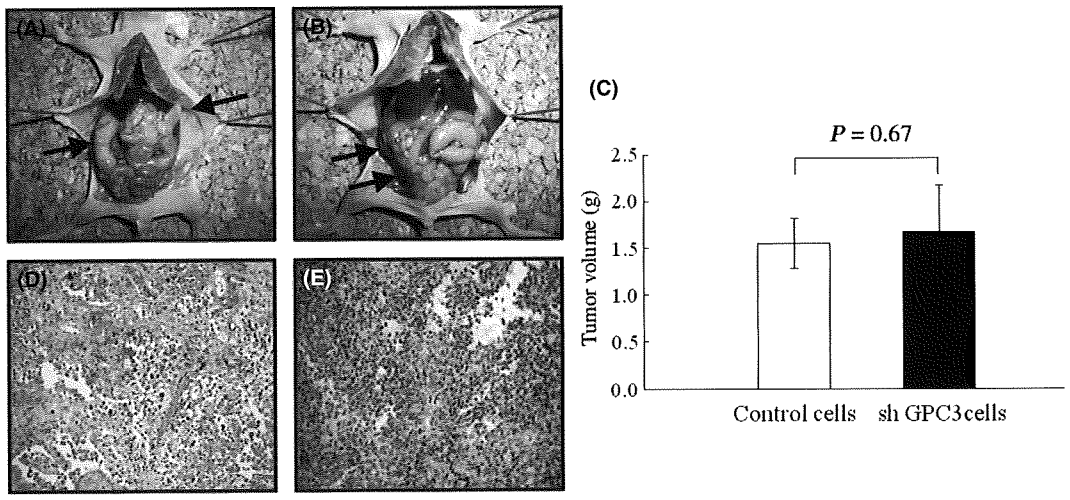


**Fig. 4.** Peritoneal progression of control cells and clear cell carcinoma cells with silenced glypican-3 expression (sh GPC3) in a nude mouse model. (A,B) Intraperitoneal appearance of mice killed 3 weeks after inoculation with control (A) and sh GPC3 (B) cells. Arrows show peritoneal dissemination. (C) Tumor volume of control and sh GPC3 cells. (D,E) Immunoreactivity of GPC3 in peritoneal dissemination. (D) Control cells. (E) sh GPC3 cells.



doi: 10.1111/j.1349-7006.2009.01382.x

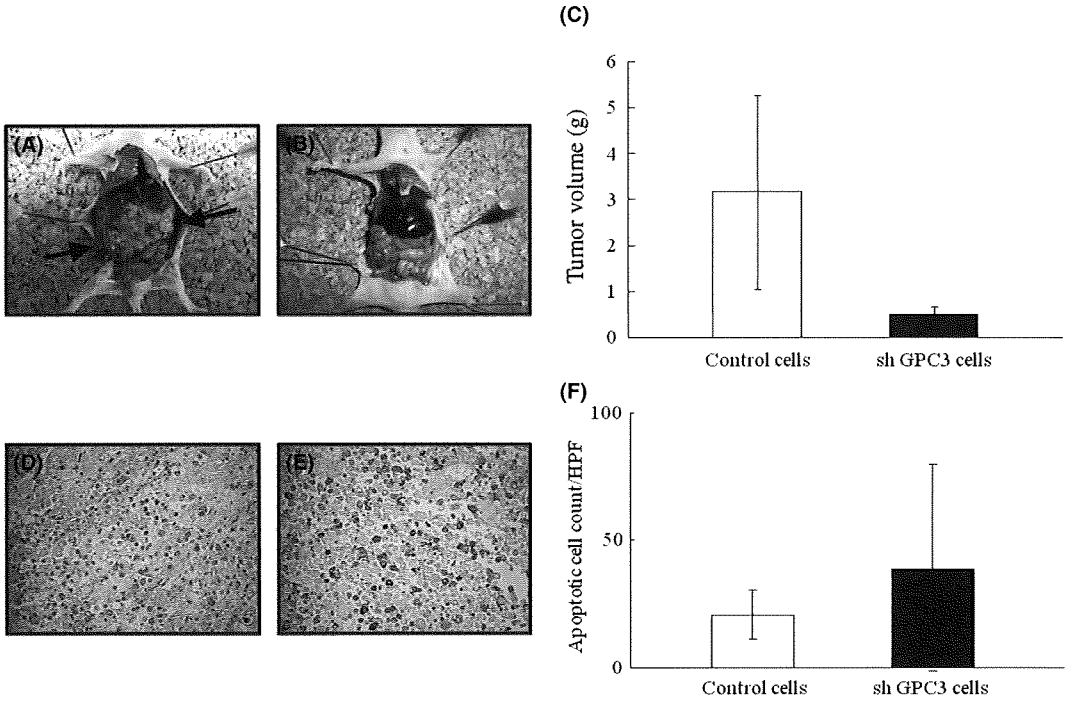


**Fig. 5.** Effect of paclitaxel treatment on the peritoneal progression of control cells and clear cell carcinoma cells with silenced glypican-3 expression (sh GPC3) in a nude mouse model. (A,B) Intraperitoneal appearance of mice killed 2 weeks after the last paclitaxel treatment. Arrows show peritoneal dissemination. (A) Control cells. (B) sh GPC3 cells. (C) Tumor volume of control and sh GPC3 cells. (D,E) Evaluation of apoptotic cells by TUNEL staining. (D) Control cells. (E) sh GPC3 cells. (F) Apoptotic cell count/high power field (HPF).

first to successfully establish the stable knockdown of a GPC3 expressing human cancer cell line using an sh RNA technique, using the CCC cell line KOC-7c, and revealed the functional implications of GPC3 in the tumor phenotype both *in vitro* and *in vivo*. Although GPC3 was not associated with the proliferation and migration potential of the CCC cell line, the sh RNA-mediated suppression of GPC3 protein expression is associated with a significant restoration of the sensitivity of CCC cells to paclitaxel. KOC-7c was the most resistant to paclitaxel of the CCC cell lines, but some serous carcinoma cell lines were more resistant to paclitaxel than KOC-7c. This suggests that the resistance to paclitaxel of serous carcinoma cell lines is due to other mechanisms, such as class III β tubulin or MDR-1, and not GPC3. The tumor volume in the control mouse peritoneum was significantly larger than in the sh GPC3 mouse. However, the evaluation of apoptosis using the TUNEL method showed no significant differences between the sh GPC3 cell xenograft and control groups after paclitaxel treatment. It may be that the observation period after paclitaxel treatment is so long that paclitaxel-resistant cells survived. Furthermore, individual differences between mice might have been too large. It has been shown that the GPC3 encoding gene is mutated in patients with Simpson–Golabi–Behmel syndrome,[7] a disorder characterized by pre- and postnatal overgrowth and various visceral and skeletal dysmorphisms. Some of these dysmorphisms could be the result of a deficiency in growth inhibition or programmed cell death. Indeed, it has been shown that GPC3 is able to induce apoptosis in a cell-specific manner.[23] GPC3 induced programmed cell death in rat mesothelioma and human breast cancer cells, but not in human colon carcinoma cells or murine NIH3T3 fibroblasts. GPC3 probably maintains the homeostatic balance between cell growth and cell death, which is ultimately the main pharmacological target of cell death-inducing antitumor agents, including paclitaxel.

Recently, GPC3 was shown to be involved in atypical multidrug resistance in gastric cancer cells. The suppression of GPC3 expression by an anti-GPC3 ribozyme not only restored sensitivity to mitoxantrone but also attenuated cross-resistance to etoposide.[20] Furthermore, the degree of drug resistance correlated with the level of GPC3 mRNA.

There is increasing evidence that GPC3 is an effective immunotherapeutic target in the treatment of GPC3 expressing cancers. Previous reports indicated that GPC3 was an effective target antigen for immunotherapy in hepatocellular carcinoma, and melanoma, raising the possibility that GPC3 peptides may be applicable to cancer immunotherapy for GPC3 overexpressing tumors.[24–26] Phase I clinical trials of immunotherapy targeting GPC3 in hepatocellular carcinoma patients is ongoing.

In conclusion, we have shown that the suppression of GPC3 in CCC cells restored paclitaxel sensitivity *in vitro*. Furthermore, the present study clearly showed the therapeutic potential of GPC3 inhibition *in vivo*. Taken together, our data could support the use of GPC3-targeted therapies for CCC patients. We suggest that therapy targeting to GPC3 may be a novel treatment strategy that could potentially help to prevent the appearance, progression, and/or recurrence of CCC.

## Abbreviations

| | |
|---|---|
| CCC | clear cell carcinoma |
| EOC | epithelial ovarian carcinoma |
| MDR-1 | multi-drug resistance gene |
| PI | propidium iodide |
| sh | short hairpin |

## References


1 Bristow RE, Montz FJ, Lagasse LD, Leuchter RS, Karlan BY. Survival impact of surgical cytoreduction in stage IV epithelial ovarian cancer. *Gynecol Oncol* 1999; **72**: 278–87.
2 Markman M, Liu PY, Wilczynski S *et al.* Phase III randomized trial of 12 versus 3 months of maintenance paclitaxel in patients with advanced ovarian cancer after complete response to platinum and paclitaxel-based chemotherapy: a Southwest Oncology Group and Gynecologic Oncology Group trial. *J Clin Oncol* 2003; **21**: 2460–5.
3 McGuire WP, Hoskins WJ, Brady MF *et al.* Cyclophosphamide and cisplatin compared with paclitaxel and cisplatin in patients with stage III and stage IV ovarian cancer. *N Engl J Med* 1996; **334**: 1–6.
4 Pectasides D, Fountzilas G, Aravantinos G *et al.* Advanced stage clear-cell epithelial ovarian cancer: the Hellenic Cooperative Oncology Group experience. *Gynecol Oncol* 2006; **102**: 285–91.
5 Sugiyama T, Kamura T, Kigawa J *et al.* Clinical characteristics of clear cell carcinoma of the ovary: a distinct histologic type with poor prognosis and resistance to platinum-based chemotherapy. *Cancer* 2000; **88**: 2584–9.
6 Kennedy AW, Biscotti CV, Hart WR, Webster KD. Ovarian clear cell adenocarcinoma. *Gynecol Oncol* 1989; **32**: 342–9.
7 Filmus J, Selleck SB. Glypicans: proteoglycans with a surprise. *J Clin Invest* 2001; **108**: 497–501.
8 Desbordes SC, Sanson B. The glypican Dally-like is required for Hedgehog signalling in the embryonic epidermis of Drosophila. *Development* 2003; **130**: 6245–55.
9 Hagihara K, Watanabe K, Chun J, Yamaguchi Y. Glypican-4 is an FGF2-binding heparan sulfate proteoglycan expressed in neural precursor cells. *Dev Dyn* 2000; **219**: 353–67.
10 Ohkawara B, Yamamoto TS, Tada M, Ueno N. Role of glypican 4 in the regulation of convergent extension movements during gastrulation in Xenopus laevis. *Development* 2003; **130**: 2129–38.
11 Song HH, Shi W, Filmus J. OCI-5/rat glypican-3 binds to fibroblast growth factor-2 but not to insulin-like growth factor-2. *J Biol Chem* 1997; **272**: 7574–7.
12 Tsuda M, Kamimura K, Nakato H *et al.* The cell-surface proteoglycan Dally regulates Wingless signalling in Drosophila. *Nature* 1999; **400**: 276–80.
13 Toretsky JA, Zitomersky NL, Eskenazi AE *et al.* Glypican-3 expression in Wilms tumor and hepatoblastoma. *J Pediatr Hematol Oncol* 2001; **23**: 496–9.
14 Yamauchi N, Watanabe A, Hishinuma M *et al.* The glypican 3 oncofetal protein is a promising diagnostic marker for hepatocellular carcinoma. *Mod Pathol* 2005; **18**: 1591–8.
15 Maeda D, Ota S, Takazawa Y *et al.* Glypican-3 expression in clear cell adenocarcinoma of the ovary. *Mod Pathol* 2009; **27**: 894–904.
16 Stadlmann S, Gueth U, Baumhoer D, Moch H, Terracciano L, Singer G. Glypican-3 expression in primary and recurrent ovarian carcinomas. *Int J Gynecol Pathol* 2007; **26**: 341–4.
17 Zynger DL, Everton MJ, Dimov ND, Chou PM, Yang XJ. Expression of glypican 3 in ovarian and extragonadal germ cell tumors. *Am J Clin Pathol* 2008; **130**: 224–30.
18 Kajiyama H, Kikkawa F, Khin E, Shibata K, Ino K, Mizutani S. Dipeptidyl peptidase IV overexpression induces up-regulation of E-cadherin and tissue inhibitors of matrix metalloproteinases, resulting in decreased invasive potential in ovarian carcinoma cells. *Cancer Res* 2003; **63**: 2278–83.
19 Kajiyama H, Shibata K, Terauchi M *et al.* Neutral endopeptidase 24.11/CD10 suppresses progressive potential in ovarian carcinoma in vitro and in vivo. *Clin Cancer Res* 2005; **11**: 1798–808.
20 Wichert A, Stege A, Midorikawa Y, Holm PS, Lage H. Glypican-3 is involved in cellular protection against mitoxantrone in gastric carcinoma cells. *Oncogene* 2004; **23**: 945–55.
21 Chevillard S, Pouillart P, Beldjord C *et al.* Sequential assessment of multidrug resistance phenotype and measurement of S-phase fraction as predictive markers of breast cancer response to neoadjuvant chemotherapy. *Cancer* 1996; **77**: 292–300.
22 Hari M, Yang H, Zeng C, Canizales M, Cabral F. Expression of class III beta-tubulin reduces microtubule assembly and confers resistance to paclitaxel. *Cell Motil Cytoskeleton* 2003; **56**: 45–56.
23 Gonzalez AD, Kaya M, Shi W *et al.* OCI-5/GPC3, a glypican encoded by a gene that is mutated in the Simpson-Golabi-Behmel overgrowth syndrome, induces apoptosis in a cell line-specific manner. *J Cell Biol* 1998; **141**: 1407–14.
24 Komori H, Nakatsura T, Senju S *et al.* Identification of HLA-A2- or HLA-A24-restricted CTL epitopes possibly useful for glypican-3-specific immunotherapy of hepatocellular carcinoma. *Clin Cancer Res* 2006; **12**: 2689–97.
25 Motomura Y, Senju S, Nakatsura T *et al.* Embryonic stem cell-derived dendritic cells expressing glypican-3, a recently identified oncofetal antigen, induce protective immunity against highly metastatic mouse melanoma, B16-F10. *Cancer Res* 2006; **66**: 2414–22.
26 Nakatsura T, Komori H, Kubo T *et al.* Mouse homologue of a novel human oncofetal antigen, glypican-3, evokes T-cell-mediated tumor rejection without autoimmune reactions in mice. *Clin Cancer Res* 2004; **10**: 8630–40.




doi: 10.1111/j.1349-7006.2009.01382.x

Cancer Science
The official journal of the Japanese Cancer Association JCA

# Expression of podoplanin, CD44, and p63 in squamous cell carcinoma of the lung

Yoshihisa Shimada,[1,2,3] Genichiro Ishii,[1] Kanji Nagai,[2] Naho Atsumi,[1] Satoshi Fujii,[1] Atsushi Yamada,[1] Yuki Yamane,[1,2] Tomoyuki Hishida,[2] Mitsuyo Nishimura,[2] Junji Yoshida,[2] Norihiko Ikeda[3] and Atsushi Ochiai[1,4]

[1]Pathology Division, Research Center for Innovative Oncology, National Cancer Center Hospital East, Kashiwa, Chiba; [2]Thoracic Oncology Division, National Cancer Center Hospital East, Kashiwa, Chiba; [3]Department of Surgery, Tokyo Medical University, Tokyo, Japan

(Received May 31, 2009/Revised July 02, 2009/Accepted July 07, 2009/Online publication August 13, 2009)

**Recent molecular biological studies have identified podoplanin as a candidate cancer stem cell (CSC) marker in squamous cell carcinoma (SqCC). The purpose of this study was to examine the expression pattern of podoplanin, and the other stem cell markers CD44 and p63, and their relationship to clinico-pathological features including survival in pulmonary SqCC. We examined histologically the expression of podoplanin, CD44, and p63 in 162 consecutive SqCC by immunostaining. Podoplanin expression was observed in 107 (66%) tumors, CD44 in 145 (89.5%), and p63 in 151 (93.2%), respectively. In 95.3% of the podoplanin-positive tumors, tumor cells showing strong expression were localized in the periphery of the tumor nests. However, this peripheral localization was observed in only 55.9% of the CD44-positive and 43% of p63-positive tumors. In 88.8% of the podoplanin-positive tumors, positive cells were localized more peripherally in the tumor nests than CD44- or p63-positive cells and when CD44 and p63 expressions were compared in these podoplanin-positive tumors, p63-positive layers in the periphery of the tumor nests were broader compared to CD44-positive layers. These findings suggest tumor cells are aligned in the "hierarchical distribution pattern" according to the expression of these three markers. Patients who had podoplanin-positive tumors with the "hierarchical pattern" resulted in significantly better overall survival than those who had podoplanin-negative tumors ($P = 0.043$). These results suggest that podoplanin expression would reflect the most immature status in the differentiation process of SqCC, and SqCC with hierarchical expression would be a well-organized tumor group with lower biological aggressiveness based on the CSC concept. (*Cancer Sci* 2009; 100: 2054–2059)**

Lung cancer is the leading cause of cancer mortality worldwide, and two main types of non-small-cell lung carcinoma (NSCLC), adenocarcinoma and squamous cell carcinoma (SqCC), account for over half the cases of lung cancer. There have been recent advances in molecularly targeted agents for the treatment of pulmonary adenocarcinoma, but not much progress has been made in the treatment of SqCC,[1–3] and the molecular mechanisms of SqCC are not completely understood.

Considering that the components of SqCC are heterogeneous and that its histology and marker expression are similar to those of normal epithelium, it suggests a ''developmental hierarchy''. Based on the concept that stem cells sit at the top of the developmental hierarchy, the cells at the basal (peripheral) region of SqCC nests may possess stem-cell-like properties. The notion that within established tumor, the great majority of the cancer cells cannot sustain the lesion and only a few cells, cancer stem cells (CSCs), are tumorigenic and possess the metastatic phenotype is CSC hypothesis. CSCs, a very small population of specialized cells, have self-renewal and extensively proliferative characteristics to sustain tumor formation.[4,5] Recent molecular biological studies have identified podoplanin, CD44, and p63 as candidate stem cell markers in normal squamous epithelium and SqCC.[6–8]

Podoplanin is a mucin-like transmembrane glycoprotein that is highly and specifically expressed in lymphatic endothelial cells.[9] Podoplanin on cancer cells has been shown to act as a platelet-aggregation factor and cell–cell adhesion promoter,[10] and induction of expression of PA2.26, a homologue of human podoplanin, in mouse epidermal cells and tumor cells has been shown to be related to increased cell migration and malignant transformation.[11] In addition, we have previously reported that podoplanin is a novel marker to enrich tumor-initiating cells with stem-cell-like properties in SqCC *in vivo* and *in vitro*. Using the human SqCC cell line A431, sorted podoplanin-positive cells have higher colony formation and tumorigenicity than podoplanin-negative cells, and xenografted tumors derived from podoplanin-positive cells are similar to those in human oral SqCC tissue and normal epithelium.[6]

The cell surface glycoprotein CD44 is involved in cell migration and cell adhesion. CD44 has been found to support anchorage-independent growth *in vitro* and tumor growth and metastasis in experimental models of solid cancer.[12] $CD44^+$ cells in breast and lung carcinoma, and head and neck SqCC, have been shown to possess the CSC properties of self-renewal and differentiation.[8,13–15]

p63, a homologue of the tumor suppressor p53, plays a crucial role in initiating epithelial stratification during development and in maintaining epidermal structures, including in the oral mucosa, skin, teeth, and other sites, and p63 has been shown to be a specific marker of human corneal and squamous epithelial stem cells.[7,16–18] The human *p63* gene codes for at least six protein isoforms as a result of initiation of transcription at two different promoter sites that contain (TA) or lack (ΔN) a transactivation domain. The isoforms have different functions and form complicated networks in different systems.[7,15,19]

The purpose of this study was to examine the expression pattern of podoplanin, CD44, and p63, and their implication for clinico-pathological features in pulmonary SqCC.

## Materials and Methods

**Patients.** During the period from January 1998 to December 2003, a total of 1279 patients underwent surgical resection for primary lung cancer at the National Cancer Center Hospital East, Chiba, Japan, and we reviewed the cases of the 167 consecutive patients in whom complete resection of pulmonary SqCC had been possible. All patients signed the Institutional Review Board–approved informed consent form. Staging was performed according to the International Union Against Cancer's tumor-node-metastasis (TNM) classification. The tumors were histologically subtyped and graded according to the third

[4]To whom correspondence should be addressed. E-mail: aochiai@east.ncc.go.jp



doi: 10.1111/j.1349-7006.2009.01295.x